

SOLID STATE SPECTROSCOPY,  
INFRARED ABSORPTION OF DECABORANE

Thesis for the Degree of M. S.  
MICHIGAN STATE UNIVERSITY

David T. Somerville

1963

THESIS



## ABSTRACT

### SOLID STATE SPECTROSCOPY: INFRARED ABSORPTION OF DECABORANE

by David T. Somerville

The infrared absorption spectrum of decaborane ( $B_{10}H_{14}$ ) is studied in the sodium-chloride range ( $4000 - 667 \text{ cm}^{-1}$ ) in the vapor, in solution, and in the solid, as an ancillary study in a program on the interaction of electromagnetic radiation with lattice vibrations. Particular attention is paid to the changes in the absorption spectrum near  $2600 \text{ cm}^{-1}$ , the region of absorption corresponding to the stretching mode of singly-bonded hydrogen atoms in the decaborane molecule, because it is a mode likely to be affected by being built into the lattice. The spectra in the vapor and in solution were obtained by standard techniques. For the solid, various methods were tried; pelleting and evaporation gave suitable spectra.

The detailed molecular and crystal structure of decaborane is described in order to provide a basis for interpreting the changes in the spectrum in going from one phase to another. The rise in transmission just before an absorption maxima is interpreted in terms of the Christiansen Filter effect. Tentative explanations are given for the appearance of a shoulder on the  $2600 \text{ cm}^{-1}$  absorption band, and for

the doubling of this absorption band upon condensation of the molecules into the solid. Identification of the two minima of the doublet is based on the atomic environment of the terminal hydrogens of the molecule. Analysis of the line shape on the basis of a damped harmonic oscillator is promising for the dilute-phase spectra, but impracticable for the solid-state spectra because of the splitting of the line.



SOLID STATE SPECTROSCOPY: INFRARED ABSORPTION OF DECABORANE

By

David T. Somerville

A THESIS

Submitted to  
Michigan State University  
in partial fulfillment of the requirements  
for the degree of

MASTER OF SCIENCE

Department of Physics and Astronomy

1963

## ACKNOWLEDGMENTS

During the time the author was involved in the several phases of his research, he was ever conscious of the many people assisting him in the work. Now that the thesis is completed, he faces an arduous task to express his appreciation without appearing to be overly saccharine. Nevertheless, some individuals have provided such major contributions toward the completion of the problem that their efforts cannot be left unrecorded.

The author is indebted to Dr. Donald J. Montgomery for initially suggesting the problem and for his guidance and encouragement as the work progressed.

Thanks go to Dr. R. D. Spence and Mr. David Arnold who constructed the decaborane molecular and crystal lattice models; to Dr. R. H. Schwendeman, of the Michigan State University Chemistry Department, who made available a Perkin-Elmer Model 21 recording spectrophotometer during the early part of the studies; to Mistery Charles Randall, Sitaran Singh Jaswal, and Kwok Fai Yeung, who as members of the solid-state spectroscopy group provided assistance during several stages of the work; to Mr. Jack Carmichael who supplied the solvents for various experimental considerations; to Mr. C. Earl McKinney who assisted in the running of spectra; to Mr. Jerry J. Tomecek who prepared the

figures; and to Mr. Frank Radovich, Market Development Department, American Potash and Chemical Corporation, who supplied the decaborane used in the experimental considerations.

The author also wishes to express his gratitude to the United States Air Force for supporting the solid-state-spectroscopy program, in particular,

The Solid State Science Division  
Air Force Office of Scientific Research  
Office of Aerospace Research  
United States Air Force  
Contract No. AF 49(638)-622  
Grant No. AFOSR 62-37

Some of the work was facilitated by the availability of certain supplies and equipment from a related project sponsored by the Metallurgy and Materials Branch, Division of Research, United States Atomic Energy Commission.

Finally, he should like to acknowledge, though in a very inadequate manner, the constant help furnished by his wife, Joyce, who typed and proofread the entire manuscript. Her faith and understanding has been a constant source of inspiration.

## TABLE OF CONTENTS

Chapter	Page
I. INTRODUCTION. . . . .	1
II. MATERIALS . . . . .	5
A. Decaborane	5
1. Chemical properties	5
2. Physical properties	8
3. Toxicity	8
B. Procurement and Analysis of Sample	9
C. Spectrophotometer	10
III. PREVIOUS CONSIDERATIONS . . . . .	11
IV. EXPERIMENTAL CONSIDERATIONS . . . . .	12
A. Safety Precautions for Decaborane	12
B. Sublimation	13
C. Evaporation	15
D. Pelleting	20
E. Mull	24
F. Solution	30
G. Vapor	34
V. RESULTS . . . . .	38

A. General Decaborane Absorption	38
B. Specific Decaborane Absorption	39
C. Christiansen Filter Effect	47
VI. INTERPRETATION OF RESULTS . . . . .	53
A. Crystal Structure	53
B. Origin of Spectra Variations	64
C. Analysis of Line Shape	69
1. Absorption by Thin Films	71
2. Absorption by Vapor and by Solution	72
D. Suggestions for Future Studies	76
BIBLIOGRAPHY. . . . .	77

## LIST OF TABLES

Table	Page
I. INFRARED ABSORPTION FREQUENCIES OF DECABORANE ( $\text{cm}^{-1}$ ) . . . . .	40
II. B-H TERMINAL STRETCHING FREQUENCIES OF DECABORANE ( $\text{cm}^{-1}$ ) . . . . .	47

## LIST OF FIGURES

Figure	Page
1. The decaborane molecule. The five boron atoms of the asymmetric unit of structure, which constitutes one-half of the molecule, are labeled with primed numerals. The remaining boron atoms are labeled with unprimed numerals. . . . .	7
2. A thin sheet of air separating two semi-infinite KBr crystals. . . . .	17
3. The interference pattern resulting from the small spacing between the substrate and the lens cover. This particular pattern was observed upon operating the spectrophotometer double-beam with a pair of KBr discs in each beam . . . . .	18
4. Absorption spectrum of a KBr pellet (blank) . . . . .	21
5. Decaborane <u>pellet</u> absorption spectrum . . . . .	23
6. Absorption spectrum of Nujol film (blank) . . . . .	25
7. Decaborane <u>solution</u> (Nujol) absorption spectrum. The increase in transmission at 2800, 2650, and 1400 $\text{cm}^{-1}$ is due to the lack of balance between the absorption of the Nujol in the reference beam and in the sample beam. . . . .	26
8. Decaborane <u>solution</u> (benzene) absorption spectrum. Only the absorption attributed to B-H terminal stretching is shown. . . . .	27
9. Decaborane <u>vapor</u> absorption spectrum. . . . .	28
10. Decaborane <u>film</u> absorption spectrum . . . . .	29
11. Absorption spectrum of benzene (blank). . . . .	32



12.	The absorption spectrum of decaborane dissolved in benzene. Most of the characteristic decaborane absorption bands are masked by strong benzene absorption. Greater amounts of benzene in the reference beam than in the sample beam cause the relative transmission to be greater than 100% in certain regions . . . . .	33
13.	Skewed absorption pattern observed in decaborane <u>vapor</u> spectrum when the gas cell is being raised to temperature during the scanning period . . . . .	35
14.	Comparison between the decaborane <u>vapor</u> absorption spectrum when the gas cell is at equilibrium (broken line), and the spectrum (solid line) when the gas cell is cooling. . . . .	37
15.	Schematic diagram of decaborane absorption spectrum . .	38
16.	B-H terminal stretching band in decaborane <u>vapor</u> absorption spectrum . . . . .	42
17.	B-H terminal stretching band in decaborane solution (Nujol) absorption spectrum. The increase in transmission on the high-frequency side of the absorption is a result of the lack of balance between the absorption of the Nujol in the reference beam and in the sample beam . . . . .	43
18.	B-H terminal stretching band in decaborane <u>solution</u> (benzene) absorption spectrum . . . . .	44
19.	B-H terminal stretching band in decaborane <u>pellet</u> absorption spectrum. The large amount of transmission on the high-frequency side of the absorption is due to a Christiansen peak (See Section V, C - <u>Christiansen Filter Effect</u> ). . . . .	45
20.	B-H terminal stretching band in decaborane <u>film</u> absorption spectrum . . . . .	46
21.	B-H terminal stretching band in <u>vapor</u> , <u>solution</u> , and <u>pellet</u> absorption spectra . . . . .	48
22.	The dispersion curves for (a) a crystal in the neighborhood of characteristic absorption, and (b) a transparent medium. . . . .	49

23.	Decaborane <u>pellet</u> and decaborane <u>vapor</u> absorption spectra (B-H terminal stretching band). A Christiansen peak appears on the high-frequency side of the absorption in the pellet spectrum; no similar transmission peak is observed in the vapor spectrum. . . . .	51
24.	(a) Disordered crystal structure, (b) Ordered crystal structure. . . . .	54
25.	Model showing one of the two possible molecular orientations in the decaborane crystal lattice. This particular orientation is specified by a <u>plus</u> in Fig. 24 . .	56
26.	Model showing one of the two possible molecular orientations in the decaborane crystal lattice. This particular orientation is specified by a <u>minus</u> in Fig. 24. Three hydrogen atoms are not observable from this view, but appear in Fig. 27 . . . . .	57
27.	Model shown in Fig. 26, except that all 14 hydrogen atoms and all 10 boron atoms can be seen. . . . .	58
28.	Decaborane ordered crystal structure-- <u>twin A</u> . . . . .	60
29.	Decaborane ordered crystal structure-- <u>twin B</u> . . . . .	61
30.	View of twin A showing the relative distance between the <u>base plane</u> molecules and the molecules in the plane translated a distance $c_0/2$ from the <u>base plane</u> (also observed in <u>twin B</u> ) . . . . .	62
31.	Schematic diagram illustrating the arrangement of xz-layers for twin A . . . . .	63
32.	(a) Diborane, ( $B_2H_6$ ); (b) Pentaborane, ( $B_5H_9$ ); (c) Decaborane, ( $B_{10}H_{14}$ ). The four sets of B-H pairs are labeled a,b,c,d . . . . .	65
33.	Plot of $\nu_-\nu_+$ vs transmission T for decaborane vapor .	75

## I. INTRODUCTION

The study of the interaction of electromagnetic radiation with atomic and molecular systems has proved valuable to the chemist and the atomic physicist because of the information it has furnished on both the structure and the energy levels of these systems. It is the hope of the solid-state physicist that spectroscopy will play a role in his field similar to that which it has played in atomic and molecular studies.

Experimental difficulties have slowed the development of spectroscopy in advancing the understanding of phenomena in solids, in particular, of lattice vibrations. The characteristic frequencies of lattice vibrations extend far into the infrared; consequently, adequate experimental techniques could not be developed until infrared instruments of wide range and high sensitivity became available.

Two probes for the study of lattice vibrations are atomic mass and atomic force field. The dependence of lattice vibrational frequencies on the force field is complicated; in contrast, the dependence on atomic mass is simple, in the first approximation being proportional to the square root of the atomic mass.<sup>1</sup> Therefore, isotopic mass may be chosen as the probe to give results readily tested against theory. The natural procedure would be to study isotopically

impure substances by varying the isotopic composition, and to study isotopically-pure compounds by varying the isotopic mass.

Such work has been in progress in this laboratory.<sup>2,3,4,5</sup> The samples are prepared in the form of thin films evaporated on appropriate substrates. Thick single crystals would be desirable to study, but their production at varying isotopic compositions would be prohibitive in money and time. Ionic crystals are desirable because of their strong interaction with electromagnetic radiation. Light elements and/or tightly-bound elements are studied, to keep the anticipated spectral response within the range of our instruments. Lithium fluoride and lithium hydride satisfy the above conditions, and at the same time decrease the complexity of interpretation because of their simple lattice structures. The initial work consequently consisted of obtaining the far-infrared absorption spectrum of lithium fluoride ( $\text{Li}^6\text{F}^{19}$ ,  $\text{Li}^7\text{F}^{19}$ ) and lithium hydride ( $\text{Li}^6\text{H}^1$ ,  $\text{Li}^6\text{H}^2$ ,  $\text{Li}^7\text{H}^1$ ,  $\text{Li}^7\text{H}^2$ ).

Extending the general study of solid-state spectroscopy leads one to consider more complicated molecules. The stable isotopes of boron ( $\text{B}^{10}$ ,  $\text{B}^{11}$ ) are available in bulk quantities, and have a large relative mass difference. The boron hydrides, then, are natural to study, with the possibility of varying  $\text{B}^{10}$  and  $\text{B}^{11}$  as well as  $\text{H}^1$  and  $\text{H}^2$ . Since decaborane ( $\text{B}_{10}\text{H}_{14}$ ) is the only boron hydride in the form of a solid at room temperature, it was chosen to be studied first.

Unfortunately, isotopically-enriched decaborane proved difficult and expensive to obtain. The weak molecular bonding in the crystal suggested, moreover, that the lattice vibrations lie too far in the infrared to be detected by our instruments. These disadvantages, along with the high toxicity of the substance, caused the immediate direction of this work to be changed. Instead of seeing how the vibrational frequencies are altered by changing the mass of the particles of the vibrating system, we see to what extent, if any, the frequencies vary as we change the environment of the particles; that is, we investigate how the infrared absorption changes in going from the moderately-disordered surroundings in the liquid or in solution, to the highly-ordered structure in the solid, or to the completely-disordered environment in the vapor.

By observing any changes in the spectrum we may gain information concerning:

- (a) the effect of inter- and intra-molecular bonding on the formation of the lattice.
- (b) the nature of the inter-molecular forces which hold the individual molecules together in the crystal lattice.
- (c) the isomeric configurations which might be associated with different crystalline modifications.
- (d) the influence of the crystal lattice on the molecular motions.

- (e) the interaction of the more or less localized vibrations of the molecules with the lattice vibrations.

The problem becomes, therefore, to obtain the infrared absorption spectra of  $B_{10}H_{14}$  in various states, and to interpret any changes observed in the spectrum accompanying the changes in state. Interpretation will involve consideration of the absorption effects of molecular environment in the crystal lattice, a suitable comparison of the stretching vibrations to a damped harmonic-oscillator, and an analysis of transmission behavior of the solid in the regions of strong absorption in terms of the Christiansen-filter effect. To simplify interpretation, we concentrate our efforts on the absorption due to a single vibration, the B-H terminal stretching mode.

## II. MATERIALS

### A. Decaborane

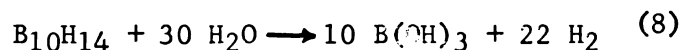
Since the end of World War II, the boron hydrides have become something more than merely an academic pastime to the inquisitive chemist. Because of their high heat of combustion and their low molecular weight, the boron hydrides and their derivatives are of interest in the propulsion field. That the boron hydrides are becoming of major interest in the missiles program is evident from the forthcoming construction of several high-energy fuel plants proposed by boron-hydride distributors. Callery Chemical Company is building a \$38 million plant for the Navy at Muskogee, Oklahoma, and a smaller privately-financed plant at Lawrence, Kansas. Olin Mathieson Chemical Corporation has completed a company-owned \$5.5 million plant at Niagara Falls, and is building a \$4.5 million plant for the Navy and a \$36 million plant for the Air Force at Model City, New York.<sup>6</sup> Decaborane itself is also useful as a catalyst, a vulcanizer, and a mild reducing agent.<sup>7</sup>

1. Chemical properties: One of the most stable of the hydrides, decaborane can be kept in air or oxygen at 50<sup>0</sup>-60<sup>0</sup>C for days without change. At 250<sup>0</sup>C in the absence of air, only 93% of the B<sub>10</sub>H<sub>14</sub> is decomposed after 24 hours. In general, it is soluble without reaction



in hydrocarbons such as hexane, benzene, and toluene. On the other hand, it may form shock-sensitive solutions in oxygenated or halogenated solvents, or in solvents containing reactive carbonyl groups.<sup>8,9</sup>

Although  $B_{10}H_{14}$  does not react with oxygen under atmospheric pressure at 60°C, it explodes when heated with oxygen in a closed system at 100°C. Hydrolysis at moderate temperatures is slight; decaborane is hydrolyzed less than 10% in 10 days at room temperature. Hydrolysis proceeds quantitatively and rapidly enough for analysis at 200°C with the following reaction:



The boron framework of the  $B_{10}H_{14}$  molecule can be described by saying that the boron atoms occupy ten of the twelve vertices of a distorted icosahedron. (Fig. 1) Boron atoms, I, IV, I', IV', form a perfect rectangle. The symmetry of the molecule is such that boron atoms V and V' lie exactly in one of the mirror planes of the molecule, and II, III, II', III', in the other mirror plane.

The surface of the molecule consists entirely of hydrogen atoms. Ten "terminal" hydrogen atoms are each joined singly to a boron atom in directions roughly corresponding to fivefold axes of the distorted icosahedral figure suggested by the boron atoms. Each of the remaining four "bridge" hydrogen atoms serves as a connection between two boron atoms. The bridging hydrogen atoms complete the surface of the

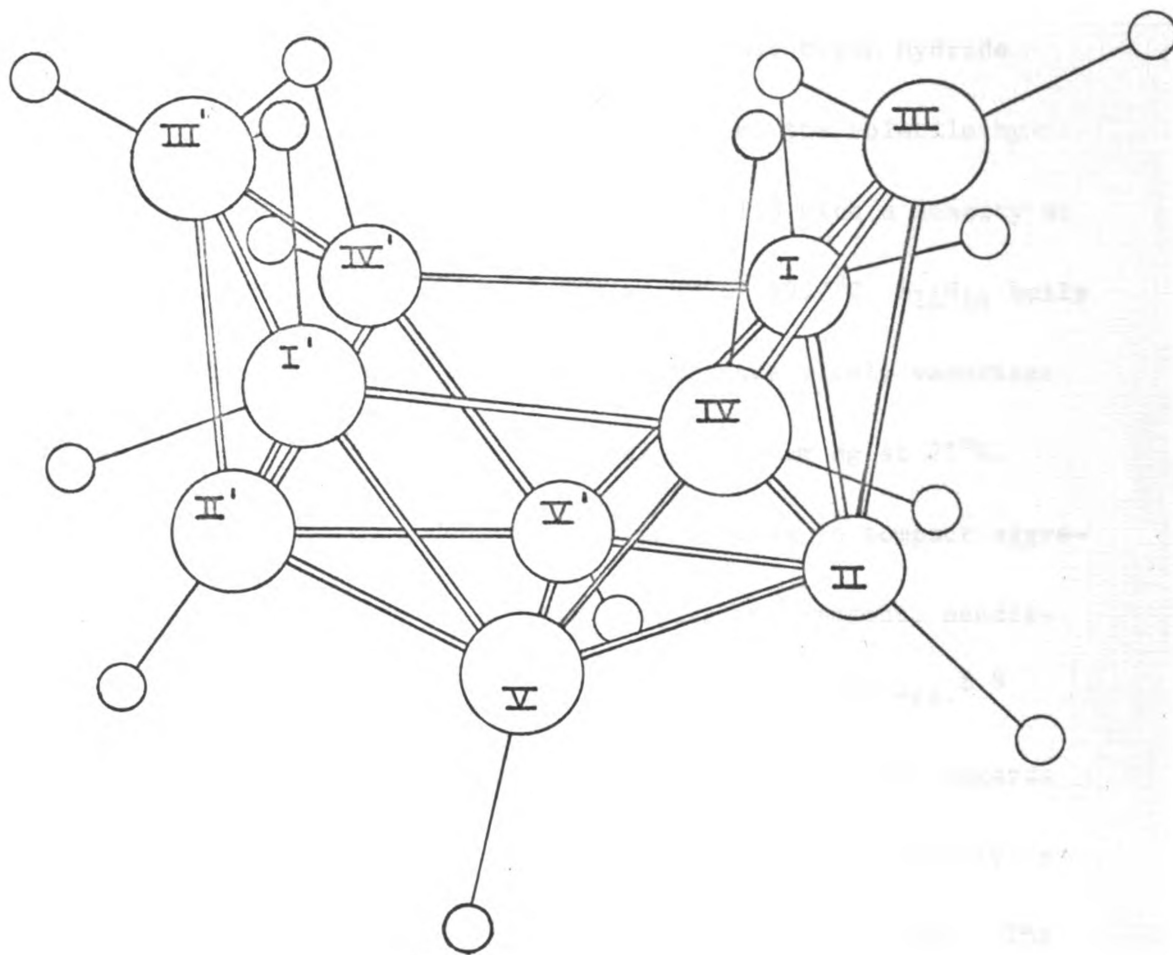


Fig. 1. - The decaborane molecule. The five boron atoms of the asymmetric unit of structure, which constitutes one-half of the molecule, are labeled with primed numerals. The remaining boron atoms are labeled with unprimed numerals.

molecule outlined by the other hydrogen atoms and also make the coordination number of each boron six.<sup>10</sup>

2. Physical properties: Decaborane, the only boron hydride solid at ordinary temperatures, is the heaviest of the volatile hydrides. It is a colorless, well-crystallized solid with a density at room temperature of 0.94 g/cm<sup>3</sup>. Melting at 99.6°-99.7°C, B<sub>10</sub>H<sub>14</sub> boils under atmospheric pressure at 213°C. The substance slowly vaporizes at room temperature, its vapor pressure being 0.05 cm Hg at 25°C. When the vapor is rapidly condensed, it crystallizes in compact aggregates. If crystallized slowly, it forms clear, transparent, needle-like crystals that may attain a length of several centimeters.<sup>8,9</sup>

3. Toxicity: Decaborane is acutely toxic, significant hazards existing by all practical routes of administration. Its toxicity is comparable to phosgene, hydrogen cyanide, and hydrogen sulfide. The inhalation hazard offered by the vapors of B<sub>10</sub>H<sub>14</sub> is such that maximum allowable atmospheric concentration for a human being in an eight-hour day is 0.3 mg/m<sup>3</sup>.<sup>7</sup> The odor is detectable at subtoxic levels, but it is not a reliable index. The hazards from skin absorption is also appreciable.<sup>11</sup>

The primary effect or action of B<sub>10</sub>H<sub>14</sub> is on the central nervous system. In addition, there is evidence of damage to the liver and kidneys; moreover changes in nucleic-acid metabolism indicate that it

is an active metabolic poison. Studies show that during periods of exposure, the effects of the poison are cumulative. The recovery of animals receiving repeated doses was markedly delayed, compared to those receiving a single dose.<sup>12</sup> To eliminate serious health hazards when working with  $B_{10}H_{14}$ , adequate control measures must be applied.

#### B. Procurement and Analysis of Sample

Isotopically-enriched decaborane is inordinately expensive. The only estimate offered to us was for 100 grams of enriched decaborane at \$6,000, exclusive of the cost of the enriched  $KBF_4$  starting material.\*

Decaborane of natural isotopic composition was supplied by the American Potash and Chemical Corporation. Their analysis is as follows:

Melting Point	97.1 - 98.2°
Decaborane (assay)	minimum 99.0%
Non-volatile impurities (at 50° and 1 mm Hg)	less than 2.0%
Metals:	
Aluminum	0.01%
Iron	0.02%
Nickel	0.05%
Silicon	0.06%
Magnesium	0.01%
Manganese	0.06%
Copper	0.01%

---

\*Personal correspondence with Mr. Frank Radovich of American Potash and Chemical Corporation.

### C. Spectrophotometer

The major part of the work was performed with a Perkin-Elmer Model 21 double-beam recording spectrophotometer with interchangeable monochromator prisms. Initially, the  $666 - 286 \text{ cm}^{-1}$  ( $15.0 - 35.0\mu$ ) range was studied with the use of cesium-bromide optics. Sodium-chloride optics, which allowed investigation in the  $4000 - 666 \text{ cm}^{-1}$  ( $2.5 - 15.0\mu$ ) region, were later introduced for the main part of the absorption studies. The Model 21 instrument permits manual or automatic programming of slit width, and variation of the recording speed and pen speed over a wide range. The scale of the recorded spectrum can be varied from a minimum of  $1 \text{ cm}/100 \text{ cm}^{-1}$  to a maximum of  $50 \text{ cm}/100 \text{ cm}^{-1}$ . To reduce atmospheric absorption, the sample area is enclosed in a metal housing, and the case is purged with dry air.

A Model 137 Perkin-Elmer KBr double-beam spectrophotometer ("Infrared") was used for work in the potassium-bromide region,  $800 - 400 \text{ cm}^{-1}$ , ( $12.5 - 25.0\mu$ ). A Beckman IR-7 spectrophotometer with cesium-iodide optics was made available to us by the Chemistry Department of Michigan State University for the range  $700 - 200 \text{ cm}^{-1}$  ( $14.3 - 50.0\mu$ ).

### III. PREVIOUS CONSIDERATIONS

The earliest studies on infrared absorption of  $B_{10}H_{14}$  were made by Keller and Johnston<sup>13</sup> in 1952. Decaborane was melted between AgCl plates, and allowed to cool. Between  $446\text{ cm}^{-1}$  and  $2624\text{ cm}^{-1}$ , 75 absorption bands in solid  $B_{10}H_{14}$  were reported.

In 1954, Bellamy<sup>14</sup> worked extensively with  $B_{10}H_{14}$  dissolved in various solvents, and found that the absorption pattern varied with the solvent. Miller and Hawthorne<sup>15</sup> observed absorption in solution and in the vapor. For  $B_{10}H_{14}$  in  $CS_2$ , they reported a broad band at  $2565\text{ cm}^{-1}$ ; for the vapor, only the lines at  $1885\text{ cm}^{-1}$  and  $1510\text{ cm}^{-1}$  are mentioned.

Decaborane in solution and in pellets was studied in the LiF region ( $0.1 - 6.0\mu$ ) by Beachell<sup>16</sup> in 1960. In solution he found a single broad band for  $B_{10}H_{14}$  at  $3.858\mu$ , but in pellets found the band split into four components at  $3.813\mu$ ,  $3.833\mu$ ,  $3.863\mu$ , and  $3.938\mu$ .

Kletz and Price<sup>17</sup> did some work concerning the change in the absorption spectrum accompanying the change of state of alkyl phenols. The formation of doublets on crystallization was reported, and was interpreted as due to association involving hydrogen bonds. A decrease in band width and an increase in absorption frequencies were observed in going from the liquid to the solid.

#### IV. EXPERIMENTAL CONSIDERATIONS

##### A. Safety Precautions for Decaborane

The extreme toxicity reported for decaborane demanded that elaborate precautions be taken in handling it. Methods were developed that controlled the harmful decaborane fumes present under normal temperature and atmospheric conditions. Samples were prepared in a dry box equipped with an exhaust pump and filter-covered openings to allow air intake (Kewaunee Scientific Equipment, Basic Laboratory Model Dry Box). The contaminated dry-box atmosphere was exhausted directly to the outside through flexible ducting. During the preparation of decaborane samples, contact with the skin was avoided by working in the dry box with externally-accessible rubber gloves sealed to the frame of the box.

The working area was kept well ventilated to decrease the concentration of fumes in case of leakage from the dry box or the sample holders. Additional precautions were taken by wearing an air-line respirator when transferring the samples from the dry box to the spectrophotometer, and when making preparations that necessitated exposure to the fumes. A KBr cover lens was used over the evaporated-film and the mull samples\* in order to prevent sublimation and reaction

---

\*Recommended in a personal communication with Harold C. Beachell, Professor of Chemistry, University of Delaware, Newark, Delaware.



with moisture when in the spectrophotometer. An object coming in contact with decaborane was thoroughly cleaned with benzene or hexane. In particular, the KBr plates used as substrates were cleaned in this way before being re-polished for subsequent use.

#### B. Sublimation

To obtain a film by sublimation, we heated a volatile substance and allowed it to deposit on a cool substrate. Sublimation in vacuo is advantageous because of the relatively free path to the substrate, which allows easier film deposition and less contamination. The toxicity of decaborane, however, required sublimation in a removable atmosphere.

The use of a vacuum system allowing controlled removal of the fumes or permitting the deposited film to be removed from the system in the dry box was first considered. A vacuum system satisfying the requirements imposed by the toxicity of decaborane was not practical because of the cost and time necessary to build such a device. The existing vacuum equipment was being used for other thin-film work and, therefore, could not be converted to the desired system. Consequently, a technique involving deposition in the dry box was attempted.

Two electrodes were attached to an insulating base upon which was placed a metal stand to hold a potassium-bromide disc acting as

a substrate; the discs were 1/8-inch thick and 1 1/8-inch in diameter. A high-resistance wire, fastened between the electrodes, cradled a molybdenum boat into which the decaborane was placed. A thin insulating strip of mica was placed between the boat and the wire to prevent both current flow through the molybdenum and localized heating of the boat. In this way the decaborane could be heated, and was expected to deposit on the KBr disc held about three inches above the molybdenum boat. To screen the substrate from any highly-volatile impurities in the decaborane powder, a movable aluminum wedge was interposed between the boat and the disc during the early part of the evaporation. All attempts to obtain a film by this method resulted in the combustion of decaborane before deposition was complete.

It became obvious that gentler heating was needed. Decaborane was placed in a weighing bottle underneath a KBr substrate held on the bottle cover by a metal spring. With the cover on the bottle, the device was a closed system that could be placed in a hot-water bath to cause the decaborane to sublime and deposit on the substrate without escape of the harmful vapors to the atmosphere. A beaker of ice was kept on top of the weighing glass to cool the substrate and minimize the re-vaporization of the deposited decaborane. The water bath consisted of a large beaker containing about one inch of water; the beaker was heated by a hot plate. The samples were removed in

the dry box and covered with a similar KBr disc when scanned in the spectrophotometer. A shortcoming of this method was the inability to shield the substrate during the early stages of sublimation.

All samples prepared in this manner failed to produce an absorption spectrum. What formed on the substrate was in fact not a film, but an agglomeration of long, needle-like crystals. The same sort of deposit resulted whether the substance was heated slowly or quickly, or if it was first dissolved in benzene and then sublimed. Removal of the beaker of ice during sublimation did not alter the result.

A layer of crystals such as that formed during the sublimation of decaborane will cause scattering as well as absorption. Scattering effects may dominate under certain conditions. But scattering may result in lower transmission than is observed. Decaborane appears to condense following sublimation in the form of long, thin crystals. Such a deposition may not absorb because of the thickness of the aggregate. Previous work by Zimmerman<sup>2</sup> with thin films of LiH may be interpreted as indicating that too thick a film will result in the failure of the material to absorb.

### C. Evaporation

When attempts to prepare a film by sublimation failed, evaporation of decaborane from solution was tried. Thiophene-free benzene,

dried over sodium, was found to be a satisfactory solvent.

In the dry box, approximately 0.5 to 0.7 mg  $B_{10}H_{14}$  was dissolved in two or three drops of  $C_6H_6$  on a KBr disc. The benzene was allowed to evaporate from the solution, while the substrate was moved in a circular path to increase the rate of evaporation and to distribute the solution evenly across the disc.

Another KBr disc was placed over the film to act as a lens cover and to keep the  $B_{10}H_{14}$  from evaporating in the radiation of the spectrophotometer. The small spacing between the substrate and lens cover produces an interference pattern superimposed on the absorption spectrum (Fig. 3).

To understand this pattern, we study a thin, non-absorbing dielectric sheet separating two semi-infinite non-absorbing dielectric media, as indicated in Fig. 2. By standard boundary-value techniques applied in electromagnetic theory, the reflection coefficient  $R$  is given by

$$R = \frac{(r_{12} + r_{23})^2 - 4r_{12}r_{23} \sin^2 \alpha_2 d}{(1 + r_{12}r_{23})^2 - 4r_{12}r_{23} \sin^2 \alpha_2 d}$$

with  $\alpha_2 \equiv \alpha \equiv 2\pi/\lambda$ , where  $\lambda$  is the wavelength within the sheet; and

$$r_{12} \equiv (\sqrt{\epsilon_1} - \sqrt{\epsilon_2}) / (\sqrt{\epsilon_1} + \sqrt{\epsilon_2}),$$

$$r_{23} \equiv (\sqrt{\epsilon_2} - \sqrt{\epsilon_3}) / (\sqrt{\epsilon_2} + \sqrt{\epsilon_3}).$$

But,

$$\sqrt{\epsilon_1} = \sqrt{\epsilon_3} = n, \text{ the refractive index of the plates,}$$

and

$$\sqrt{\epsilon_2} = 1, \text{ the refractive index of air.}$$

Then

$$r_{12} = -r_{23} \equiv r = (n - 1)/(n + 1).$$

We have

$$R = (4r^2 \sin^2 \alpha d) / [(1 - r^2)^2 + 4r^2 \sin^2 \alpha d]$$

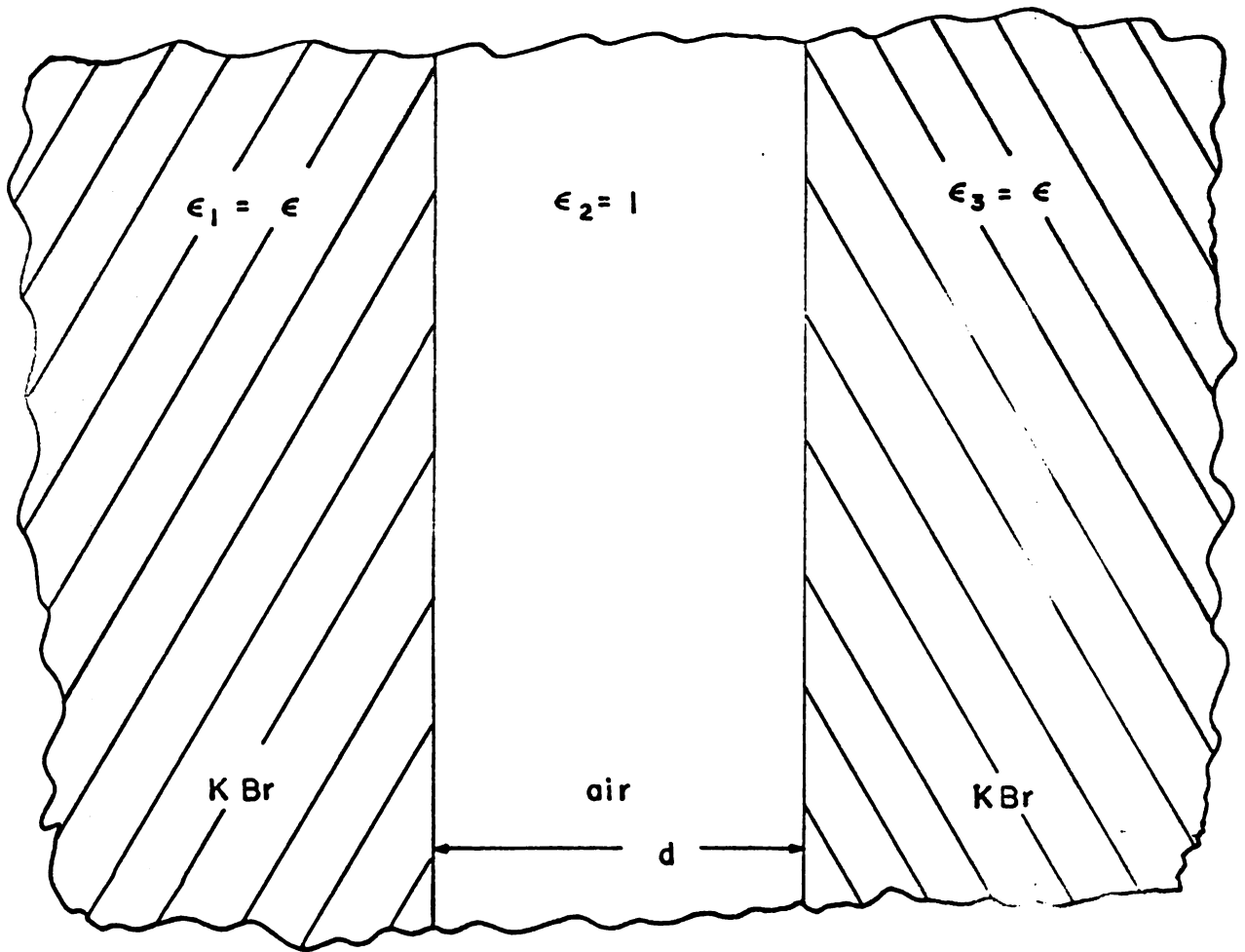


Fig. 2. - A thin sheet of air separating two semi-infinite KBr crystals.

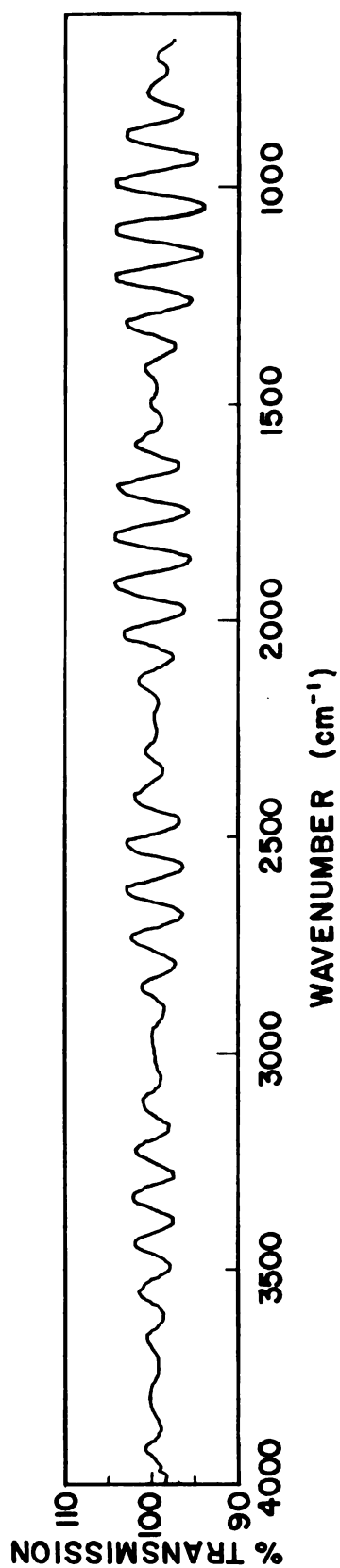


Fig. 3. - The interference pattern resulting from the small spacing between the substrate and the lens cover. This particular pattern was observed upon operating the spectrophotometer double-beam with a pair of KBr discs in each beam.

and

$$T \equiv 1 - R = (1 - r^2)^2 / [(1 - r^2)^2 + 4r^2 \sin^2 \alpha d]$$

$$= [(1 - r^2)^2 / (1 + r^4)] / [1 - (2r^2 \cos 2\alpha d) / (1 + r^4)]$$

With double-beam techniques, the recorded transmission is actually a ratio of the sample transmission to the reference transmission. We therefore are interested in the ratio of the transmission for two films differing in thickness by  $\delta$ . We write the thickness  $d$  of the thicker film as  $d_0 + \frac{1}{2}\delta$ , that of the thinner film as  $d_0 - \frac{1}{2}\delta$ , where  $d_0$  is the average thickness.

Define

$$D_+ \equiv 2\alpha (d_0 + \frac{1}{2}\delta),$$

$$D_- \equiv 2\alpha (d_0 - \frac{1}{2}\delta),$$

$$B \equiv 2r^2 / (1 + r^4).$$

Then the ratio of the transmission  $T_+$  for the thicker film to the transmission  $T_-$  for the thinner film is

$$\frac{T_+}{T_-} = \frac{1 - B \cos D_-}{1 - B \cos D_+} = (1 - B \cos D_-)(1 + B \cos D_+ + B^2 \cos^2 D_+ + \dots)$$

$$\cong 1 + B(1 + B \cos D_+)(\cos D_+ - \cos D_-)$$

to terms in  $B^2$ . For KBr,

$$r^2 = (1.53 - 1)^2 / (1.53 + 1)^2 = 0.044$$

and  $r^4 = 0.0019$ . Hence we may approximate  $B$  as

$$B \cong 2r^2 = 2(n - 1)^2 / (n + 1)^2.$$

Upon substituting the definition of  $D_+$ ,  $D_-$ ,  $B$ , and  $\alpha \equiv 2\pi/\lambda$  and replacing wavelength  $\lambda$  by wavenumber  $\mathcal{D} \equiv 1/\lambda$ , we find

$$T_+/T_- \cong$$

$$4[(n - 1)/(n + 1)]^2 \sin(4\pi d_0 \mathcal{D}) \sin(2\pi \delta \mathcal{D}) \cdot$$

$$\{1 + 2[(n - 1)/(n + 1)]^2 \cos[4\pi(d_0 + \frac{1}{2}\delta)\mathcal{D}]\}$$

that is, the transmission ratio as a function of wavenumber  $\mathcal{D}$  fluctuates above and below 100% by a maximum amount

$$4[(n - 1)/(n + 1)]^2 \sim 17.6\%$$

for the air-KBr system, upon neglecting the second-term within the braces\*. The form of the fluctuation is that of a sinusoid in  $\mathcal{D}$  with short period  $\frac{1}{2}d_0$ , amplitude-modulated by a sinusoid in  $\mathcal{D}$  with long period  $1/\delta$ .

---

\*The second-order term introduces a minor second-order short-period modulation with amplitude not exceeding 8.8% of 17.6%  $\sim 1.5\%$ .



By varying the amount of decaborane dissolved in the benzene, films of different thicknesses could be produced. The thickness was found to have no effect on the position of the absorption maxima, if indeed the film showed selective absorption at all. Hexane was also used as a solvent in the evaporation of decaborane, but the position of the absorption maxima was not affected significantly by the choice of solvent.

#### D. Pelleting

A well-known method of sample preparation in near-infrared spectroscopy of powdered substances is pelleting. In the present study, a Perkin-Elmer evacuable die was used to press a mixture of KBr and  $B_{10}H_{14}$  into a thin transparent disc, 13 mm in diameter and 0.7 to 1.0 mm in thickness. The composition of the mixture for the pellets was 0.5 mg  $B_{10}H_{14}$  mixed with 200 - 300 mg KBr. The KBr powder was of 325 mesh and 250 mesh, corresponding to screen openings of 0.0017 inch and 0.0024 inch, respectively.

Because KBr is highly hygroscopic, the elimination of moisture from a pellet is difficult. The KBr was kept above room temperature by heating the powder on a hot plate before placing it in the die. As shown in Fig. 4, water absorption is present in the pellet, but not in a region that will distort the decaborane absorption spectrum.

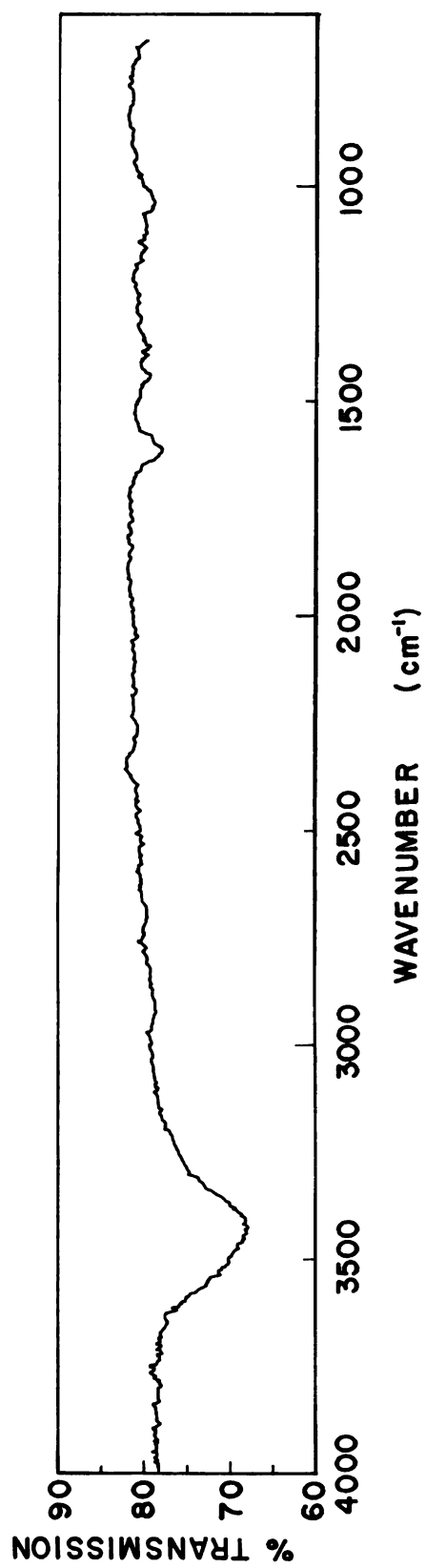


Fig. 4. - Absorption spectrum of a KBr pellet (blank).

The powders were mixed and placed into the die while they were in the dry box. The mixture was pressed into a pellet in vacuo with a Wabash Model 12-10-S hydraulic press, under pressures of approximately 6,000 lb/in<sup>2</sup> for five minutes or more.

The main disadvantage of the pellet method in the far-infrared region is lack of reproducibility in the spectra. This variability is due to the differences in particle size, and possibly to the changes resulting from the very high local temperatures and pressures developed during the formation of the pellet.<sup>18</sup> In the present investigation, however, reproducibility was not a problem when temperature and humidity were kept constant and the same mesh KBr powder was used.

Chemical reactions between the substance under study and the materials in the alkali-halide matrix must also be considered. Since high local temperatures and pressures may cause the water in the matrix to react with the decaborane, the pellet spectra were checked for boric-acid characteristic absorption bands, as recorded by Miller and Wilkens.<sup>19</sup> The strong  $\text{H}_3\text{BO}_3$  band at  $3270\text{ cm}^{-1}$  does not appear in the pellet spectra as shown in Fig. 5. The very strong absorption at  $1450\text{ cm}^{-1}$  might be present, but it would be obscured by the strong  $\text{B}_{10}\text{H}_{14}$  absorption in this region. Since the strong band at  $1195\text{ cm}^{-1}$  is missing, or so weak that it cannot be distinguished from the noise of the spectrophotometer, the amount of boric acid present must be slight.

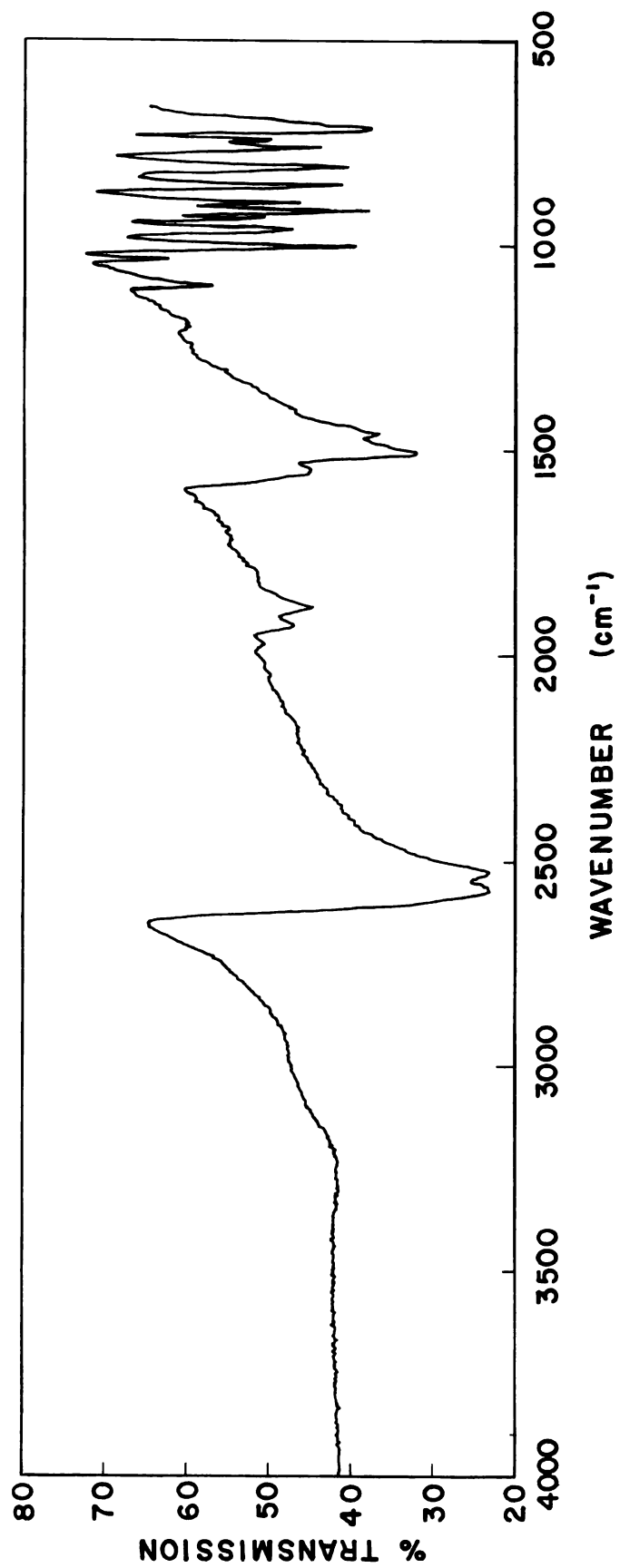


Fig. 5. - Decaborane pellet absorption spectrum.

### E. Mull

In comparing mulling and pelleting as methods of sample preparation, Baker<sup>20</sup> concluded that in combination they will yield significantly more information than will either separately. A mulling liquid must satisfy certain general requirements. It should be free from absorption bands in the spectral region of interest; it should have approximately the same refractive index as the powder outside the absorption bands, so that the amount of scattering by the powder will be small; it should have a moderate viscosity, and should mix well with the powder.<sup>18</sup> Nujol, a highly-refined mineral oil, is often satisfactory in mull preparations. Its absorption spectrum is shown in Fig. 6.

Approximately 1 mg of decaborane was mixed into a drop of Nujol on a KBr disc. The layer of the mineral oil had to be thin to minimize liquid absorption. To prepare the sample for the spectrophotometer, another KBr disc was placed on top of the mull to confine the mixture and keep the decaborane from evaporating while in the infrared radiation. A pair of KBr discs with a drop of Nujol between them was inserted in the reference beam of the spectrophotometer as compensation.

The resulting spectrum (Fig. 7) shows a single absorption band in the  $2600 - 2500 \text{ cm}^{-1}$  region, which is also found in solution and vapor spectra (Figs 8, 9). In the same region, on the other hand, pellet and film samples (Figs 5, 10) have two absorption bands. In

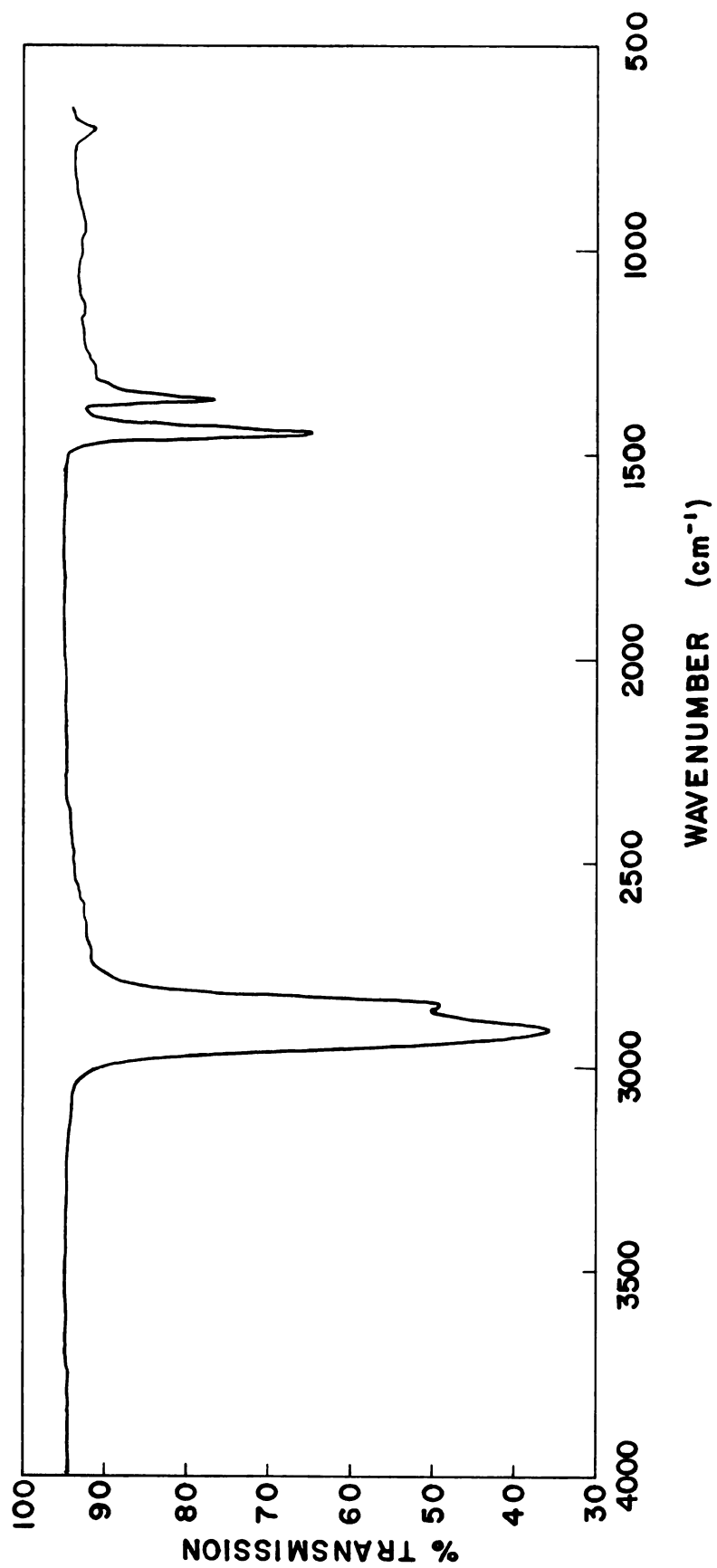


Fig. 6. - Absorption spectrum of Nujol film (blank).

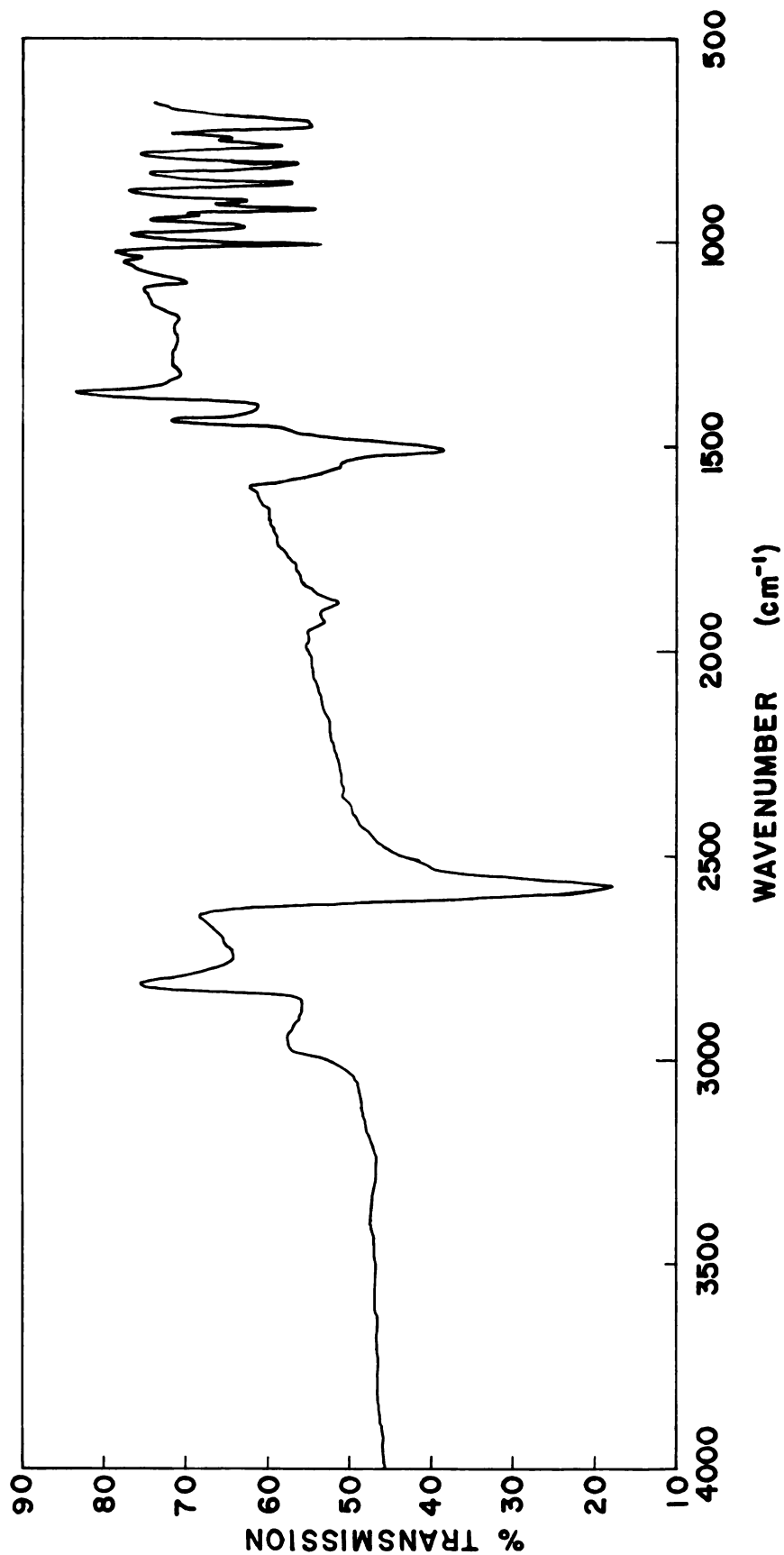


Fig. 7. - Decaborane solution (Nujol) absorption spectrum. The increase in transmission at 2800, 2650, and 1400  $\text{cm}^{-1}$  is due to the lack of balance between the absorption of the Nujol in the reference beam and in the sample beam.

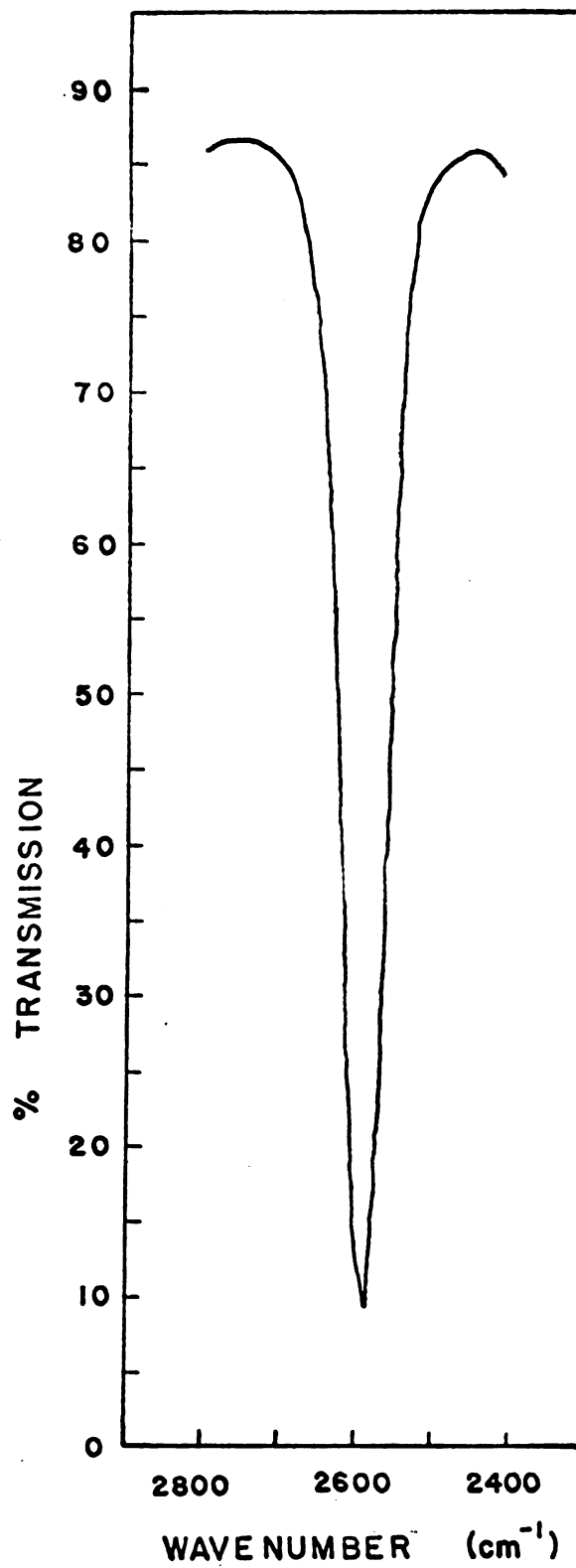


Fig. 8. - Decaborane solution (benzene) absorption spectrum. Only the absorption attributed to B-H terminal stretching is shown.



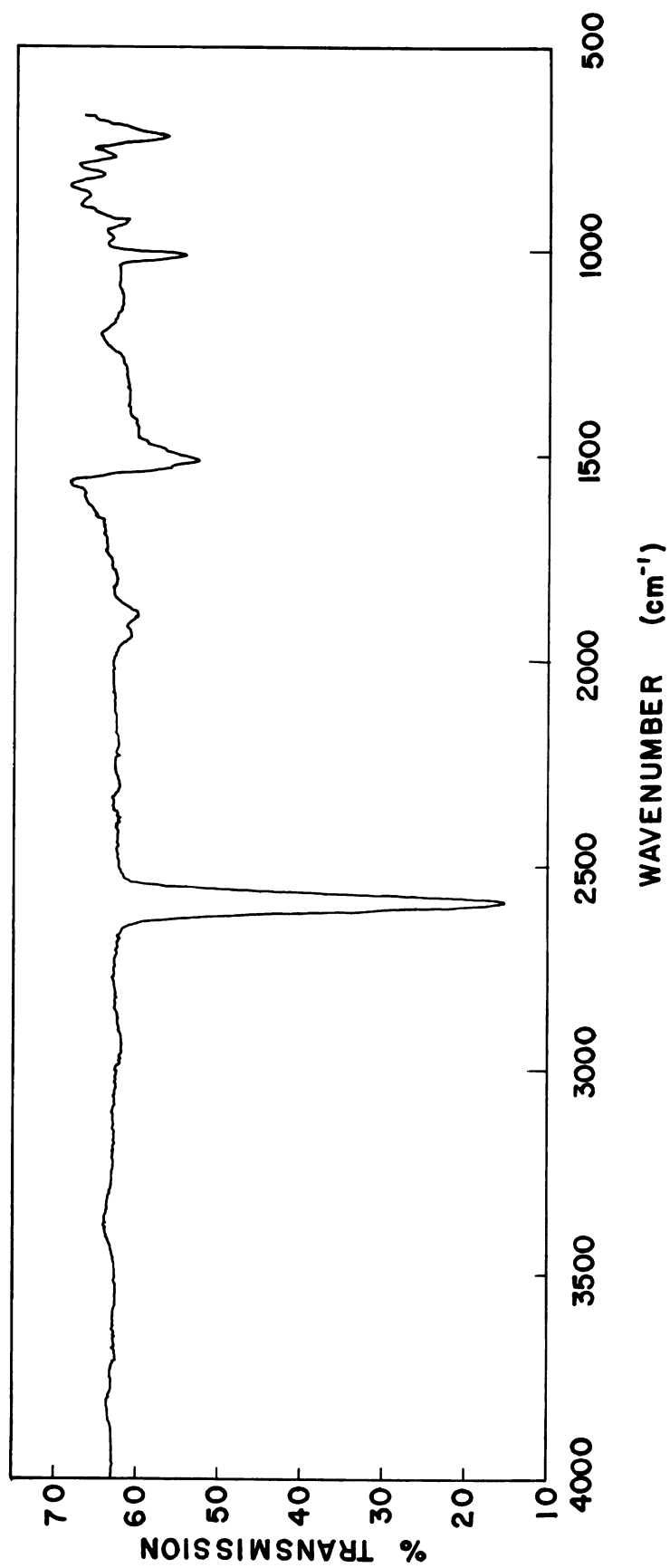


Fig. 9. - Decaborane vapor absorption spectrum.

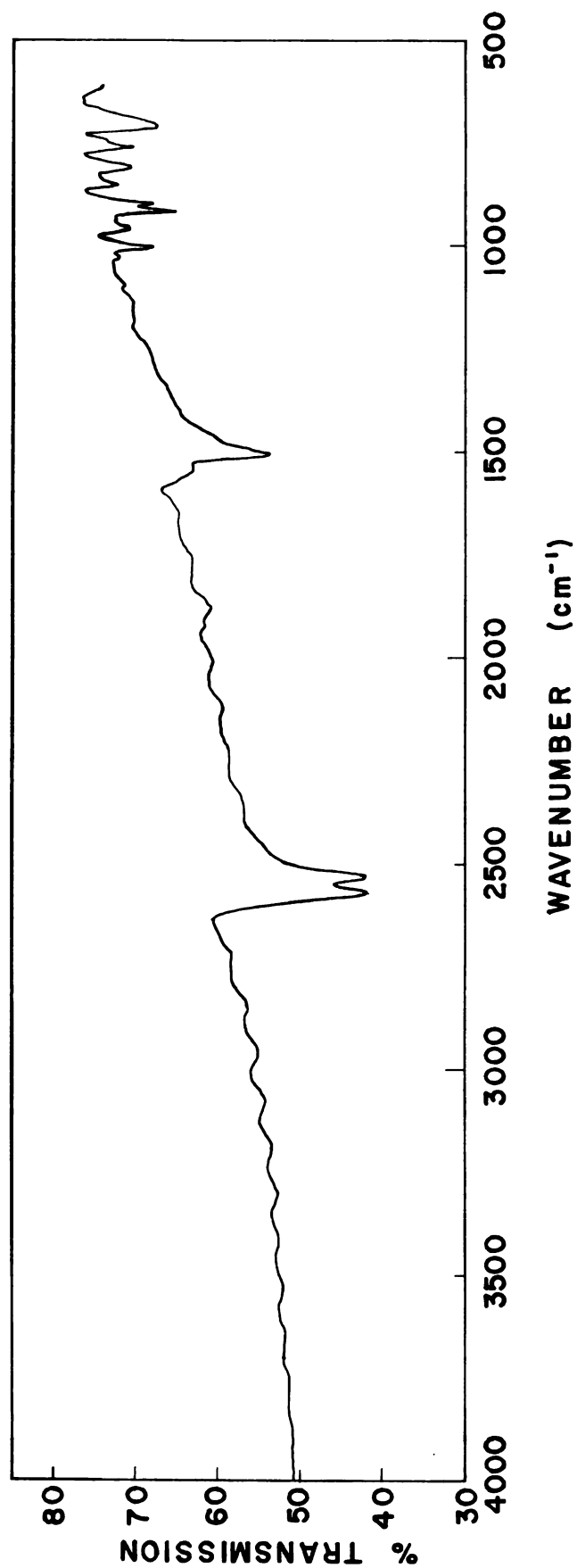


Fig. 10. - Decaborane film absorption spectrum.

view of the solubility of decaborane in hydrocarbons, it was feared that Nujol, a mixture of long-chain hydrocarbons, dissolved the  $B_{10}H_{14}$ . To study the possibility that the absorption is due to dissolved rather than suspended materials, some powder was allowed to stand in Nujol in a test tube for 64 hours. The Nujol solution was found clear, with no decaborane particles observable. A drop of the liquid was scanned, and the characteristic solution absorption was observed.

Petroleum jelly, also a mixture of long-chain hydrocarbons, gave similar results when used as a mulling substance with decaborane. For future work, we recommend that mulling agents other than long-chain hydrocarbons such as silicones be considered. The dearth of special chemical facilities for handling decaborane made such studies uneconomical in our laboratory.

#### F. Solution

Absorption studies of decaborane in solution were made with two KBr cavity-cells manufactured by the Connecticut Instrument Corporation. Thin cavities are necessary to keep the solvent absorption small. The KBr cells have 1.0 mm pathlengths and 0.068 ml volumes.

For solution spectroscopy, the solvent must not react with the solute and must not absorb in the region of interest. Carbon tetrachloride and carbon disulfide satisfy these requirements almost ideally.

But these solvents produce decaborane solutions that are reported to be shock sensitive, and whose handling requires elaborate facilities.

Benzene and hexane dissolve decaborane to form stable solutions, but the solvents themselves show some absorption close to the region of interest ( $2600\text{ cm}^{-1}$ ). Whether this absorption interferes seriously with the decaborane spectrum depends on the amount of solvent in the beam. With the KBr liquid-cell, the relatively great thickness ( $1\text{ mm} = 1000\mu$ ) results in a prohibitively great absorption with hexane. With benzene, the absorption is significant near  $2600\text{ cm}^{-1}$  (Fig. 11), but compensation by an identical benzene-filled cell in the reference beam allows its use in the study of the principal decaborane band. Most of the other bands were masked, however, by the benzene absorptions. (Fig. 12)

In the controlled atmosphere of the dry box, approximately 0.3 mg decaborane was dissolved in 2 ml benzene. The solution was put into the liquid cell with a No. 23 needle and syringe. The sample was scanned with use of double-beam techniques.

Other solution methods are suggested by the solubility of decaborane in highly viscous substances, such as long-chain hydrocarbons [Section IV, E - Mull]. With such materials, liquid cells need not be used; instead the solution is merely spread between KBr discs which are then mounted in the spectrophotometer. In this way the pathlength

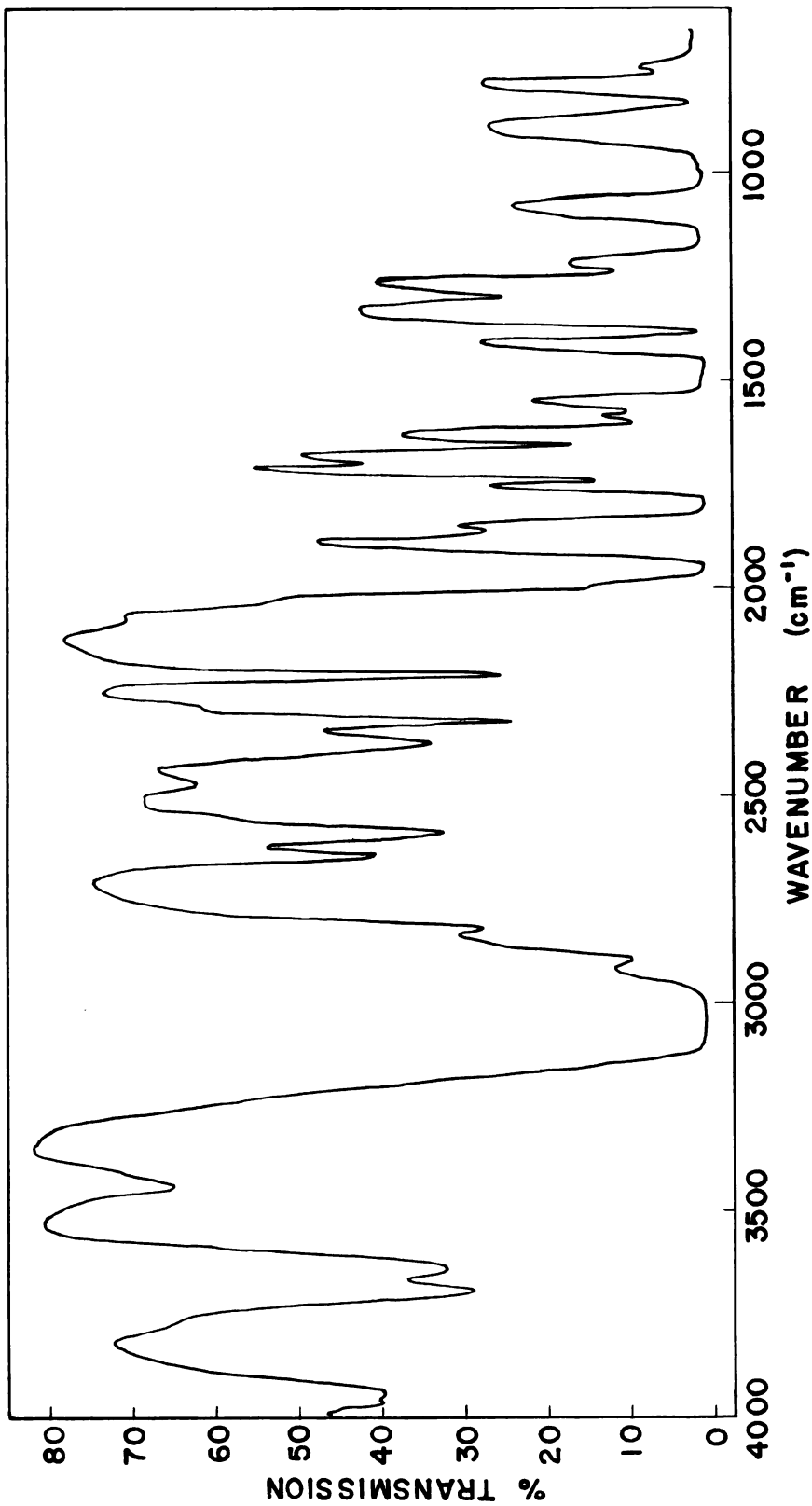


Fig. 11. - Absorption spectrum of benzene (blank).

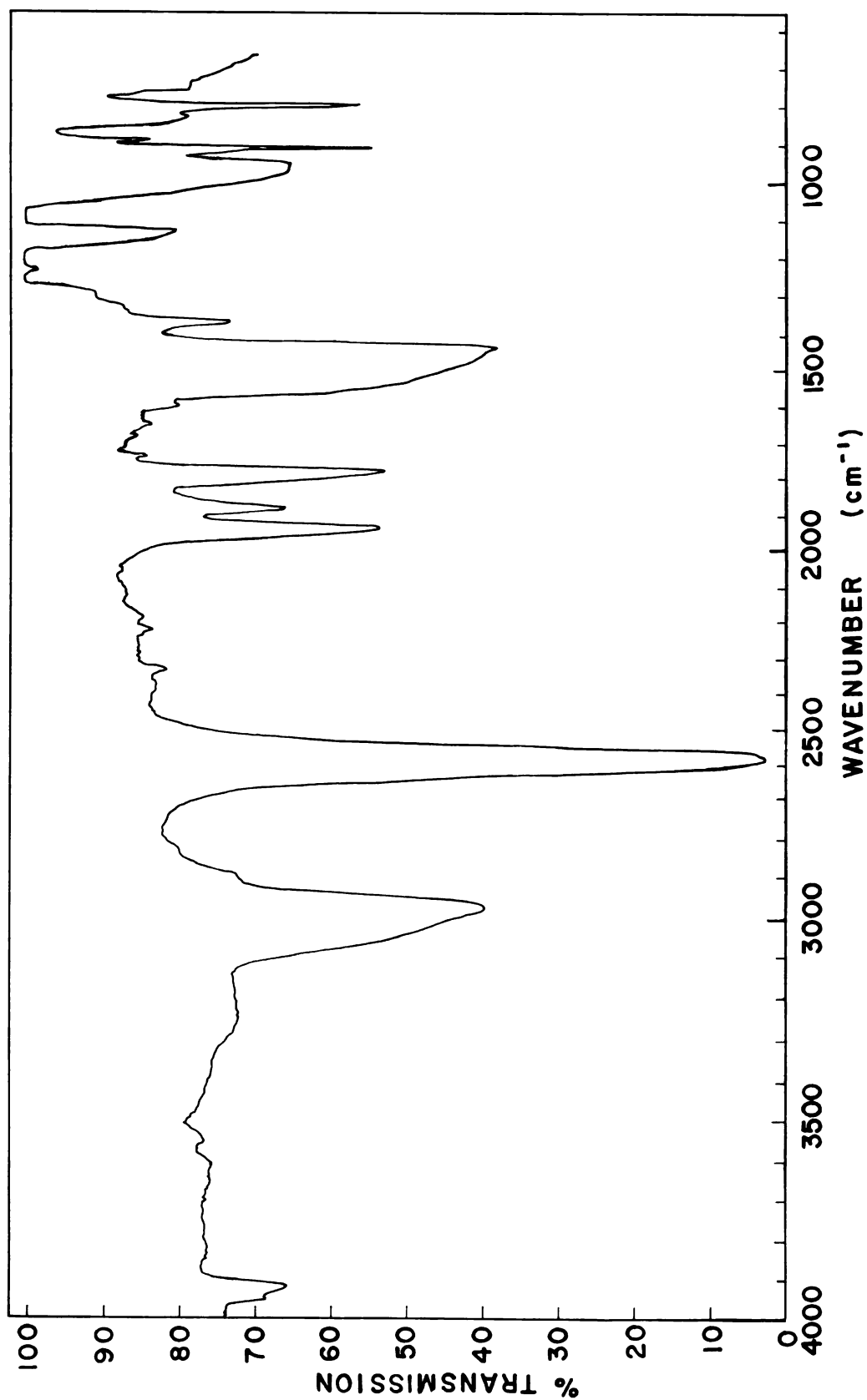


Fig. 12. - The absorption spectrum of decaborane dissolved in benzene. Most of the characteristic decaborane absorption bands are masked by strong benzene absorption. Greater amounts of benzene in the reference beam than in the sample beam causes the relative transmission to be greater than 100% in certain regions.

in the solution may be made very small, since it is determined by the thickness of the layer rather than by the fixed dimension of the cavity cell.

#### G. Vapor

Experiments on the vapor were made with the aid of a Perkin-Elmer 10-cm gas cell having KBr end-windows. Approximately 15 mg  $B_{10}H_{14}$  powder was placed in the cell. Three feet of Electrothermal "Heat by the Yard" thermal tape was placed around the gas cell to heat it and thereby vaporize the  $B_{10}H_{14}$ .

The behavior of the vapor absorption pattern during various stages of heating and cooling of the cell warrants comment. If the cell and its contents were at equilibrium, there would be no transient phenomena. It is impractical, however, to work always at equilibrium; therefore, it is necessary to understand the behavior of the material in the cell as it warms or cools. The heating causes evaporation of the solid  $B_{10}H_{14}$  at the bottom of the cell; the vapor redeposits in part on the KBr end-windows as the cell cools at the conclusion of a run. At the beginning of the following run, as the cell comes up to temperature, the deposited crystals re-evaporate, and the transmission increases as time goes on and lower wavenumbers are reached (Fig. 13). If this interpretation is correct, then in the steady state of true equilibrium,

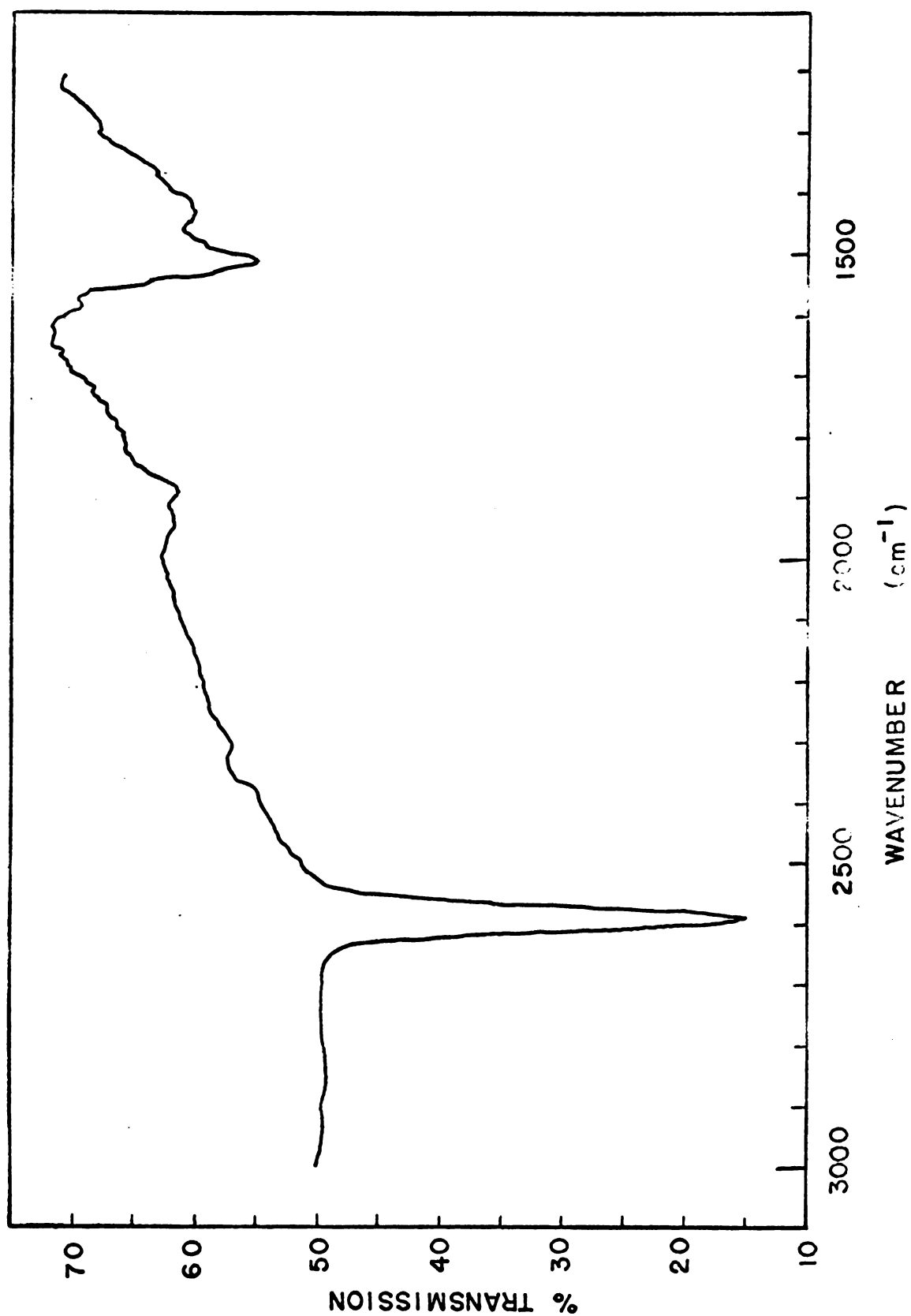


Fig. 13. - Skewed absorption pattern observed in decaborane vapor spectrum when the gas cell is being raised to temperature during the scanning period.



there should be no general rise. Such behavior is indeed observed (Fig. 9). During the cooling of the cell, there occurs a loss of structure in the  $B_{10}H_{14}$  spectrum, as well as a decrease in transmission. The loss of structure could be due to both the crystal formation on the cell windows and the smaller amount of  $B_{10}H_{14}$  vapor in the cell. The lesser degree of selective absorption resulting from crystallized decaborane is consistent with the failure to observe absorption in a thin film of  $B_{10}H_{14}$  deposited by sublimation techniques [See Section IV, B - Sublimation]. Fig. 14 compares the absorption spectrum of the gas in the heated cell with the absorption pattern after the cell has cooled.

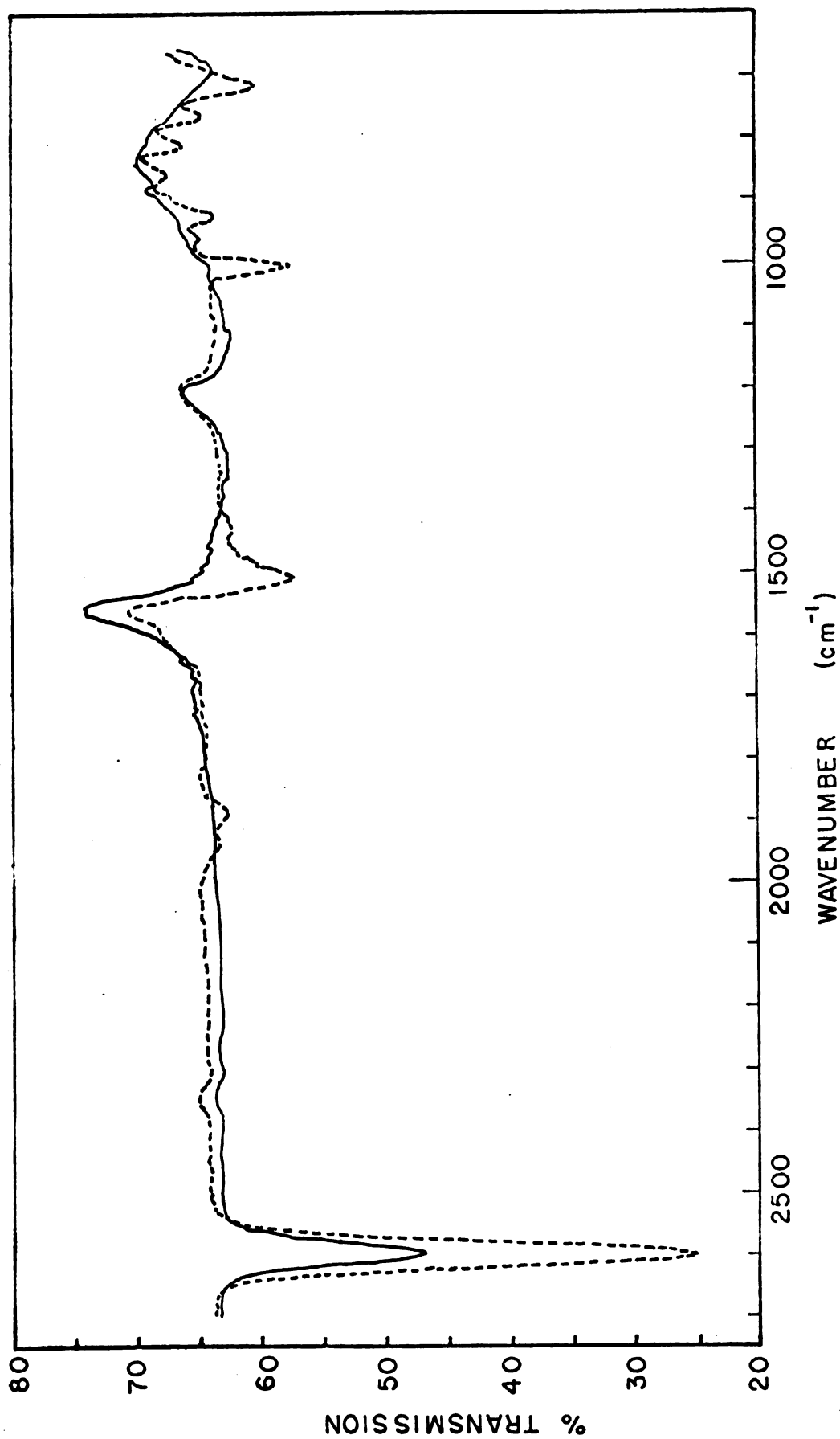


Fig. 14. - Comparison between the decaborane vapor absorption spectrum when the gas cell is at equilibrium (broken line), and the spectrum (solid line) when the gas cell is cooling.

## V. RESULTS

### A. General Decaborane Absorption

The infrared absorption spectrum of  $B_{10}H_{14}$  has four major regions of activity as indicated schematically below.

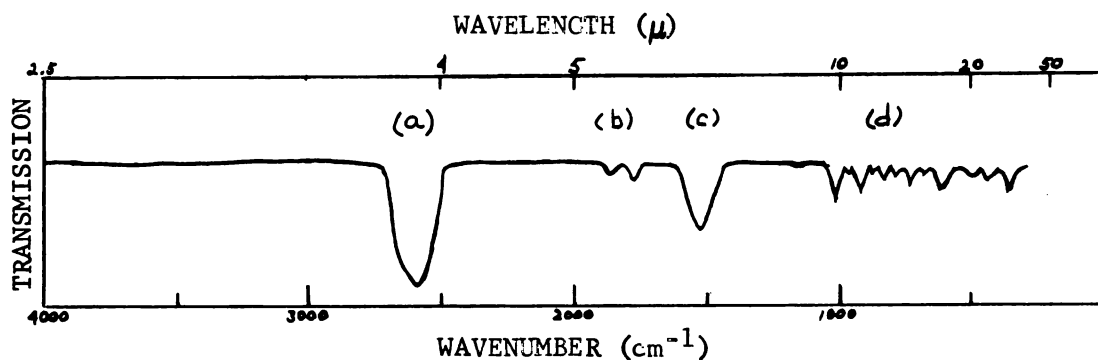


Fig. 15. - Schematic diagram of decaborane absorption spectrum.

- (a) The  $2600\text{ cm}^{-1}$  region shows very strong absorption, attributed to B-H terminal stretching\* by Hrostowski and Pimentel.<sup>21</sup>
- (b) The  $1900\text{ cm}^{-1}$  region shows two absorptions of medium intensity, attributed to B-H bridge stretching\*\* by Hrostowski and Pimentel<sup>21</sup> and by Bellamy.<sup>22</sup>
- (c) The  $1500\text{ cm}^{-1}$  region shows strong absorption, attributed to B-H bridge stretching by Shapiro et al.<sup>23</sup> They point out

---

\*This expression represents the stretching between each of the boron atoms and the hydrogen atoms singly attached thereto.

\*\*This expression represents the stretching between each of the four hydrogen atoms and the pairs of boron atoms which they bridge.

that the so-called "characteristic" bridge absorption is quite dependent on the identity of the parent boron hydride. They accordingly assign the absorptions for a series of alkyl diboranes.

- (d) The  $1010 - 350 \text{ cm}^{-1}$  region shows a highly-structured absorption attributed by Keller and Johnston<sup>13</sup> to B-B skeletal stretching ( $1100 - 400 \text{ cm}^{-1}$ ), B-B skeletal bending ( $400 - 200 \text{ cm}^{-1}$ ), and B-H terminal bending ( $600 - 800 \text{ cm}^{-1}$ ).

#### B. Specific Decaborane Absorption

The absorption data for the vapor, the solution, and the solid are listed in Table I. The results give an indication of the changes in absorption accompanying the change of state, but certain limitations in the data should be considered. Owing to the large amount of absorption by benzene, only the B-H terminal stretching band could be obtained from the benzene-solution spectrum (Fig. 8). Although the spectrum for a smear of  $\text{B}_{10}\text{H}_{14}$  in Nujol (Fig. 7) is listed as in solution, the sample could conceivably be a mixture of suspended powder and dissolved material. However, the single-band absorption at  $2575 \text{ cm}^{-1}$ , the region of interest for this investigation, favors the interpretation as solution. Four absorptions (at 1095, 1033, 917,  $742 \text{ cm}^{-1}$ ) appearing in the Nujol, the film, and the pellet spectra, are not observed in

TABLE I

INFRARED ABSORPTION FREQUENCIES OF DECABORANE ( $\text{cm}^{-1}$ )\*

<u>Film</u>	<u>Pellet</u>	<u>Solution</u> <u>(Benzene)</u>	<u>Solution</u> <u>(Nujol)</u>	<u>Vapor</u>
2572 (vs)	2568 (vs)	2587 (vs)	2575 (vs)	2587 (vs)
2531 (vs)	2528 (vs)			
1921 (vw)	1927 (m)		1928 (m)	1933 (m)
1880 (w)	1882 (m)		1881 (m)	1886 (m)
1543 (w)	1549 (m)			
1508 (s)	1508 (s)		1505 (s)	1509 (s)
	1459 (s)			
1096 (vw)	1099 (m)		1095 (m)	
1032 (vw)	1032 (m)		1033 (w)	
1005 (m)	1001 (s)		1002 (s)	1009 (s)
960 (w)	961 (s)		959 (m)	963 (w)
937 (vw)	933 (m)		934 (w)	927 (m)
918 (s)	918 (s)		917 (s)	
900 (m)	898 (m)		897 (m)	898 (vw)
853 (w)	853 (s)		853 (s)	860 (w)
809 (m)	809 (s)		808 (s)	810 (m)
762 (m)	761 (s)		762 (s)	766 (m)
744 (vw)	743 (m)		742 (m)	
711 (s)	716 (s)		713 (s)	719 (s)
	653 (w)			
623 (m)	624 (m)			
	542 (w)			
	447 (vw)			
	434 (m)			
	385 (s)			

\*Relative intensity: vs = very strong; s = strong; m = medium;  
w = weak; vw = very weak

the vapor spectrum. The apparent increase in transmission (See Section V, C - Christiansen Filter Effect) at  $1560\text{ cm}^{-1}$ ,  $1200\text{ cm}^{-1}$ , and  $840\text{ cm}^{-1}$  in the vapor spectrum (Fig. 9) indicates, however, that crystallization has occurred on the windows of the gas cell during scanning. We have suggested (See Section IV, G - Vapor) that such a deposition may destroy some of the structure in the spectrum. The vapor absorption at  $2587\text{ cm}^{-1}$  is consistent with the single-band absorption of the solutions.

Only film and pellet samples were studied at frequencies smaller than  $666\text{ cm}^{-1}$ . In particular, pellet absorption was observed in the CsBr region ( $666 - 286\text{ cm}^{-1}$ ) during the initial stages of the work. Film spectra were studied down to  $400\text{ cm}^{-1}$ , after which efforts were concentrated on the NaCl region ( $4000 - 666\text{ cm}^{-1}$ ), in particular, around  $2600\text{ cm}^{-1}$ .

To study the B-H terminal stretching band more carefully, the scale of the recording spectrum was expanded at the  $2600\text{ cm}^{-1}$  region. Table II compares the results for the two recording scales. The shift in frequency accompanying the change in recording scale seems to be within the accuracy of the spectrophotometer. The increased resolution has allowed the detection of a shoulder appearing at  $2600$  or  $2601\text{ cm}^{-1}$  in all samples (Figs 16 - 20).

The following are the main features of the behavior of the

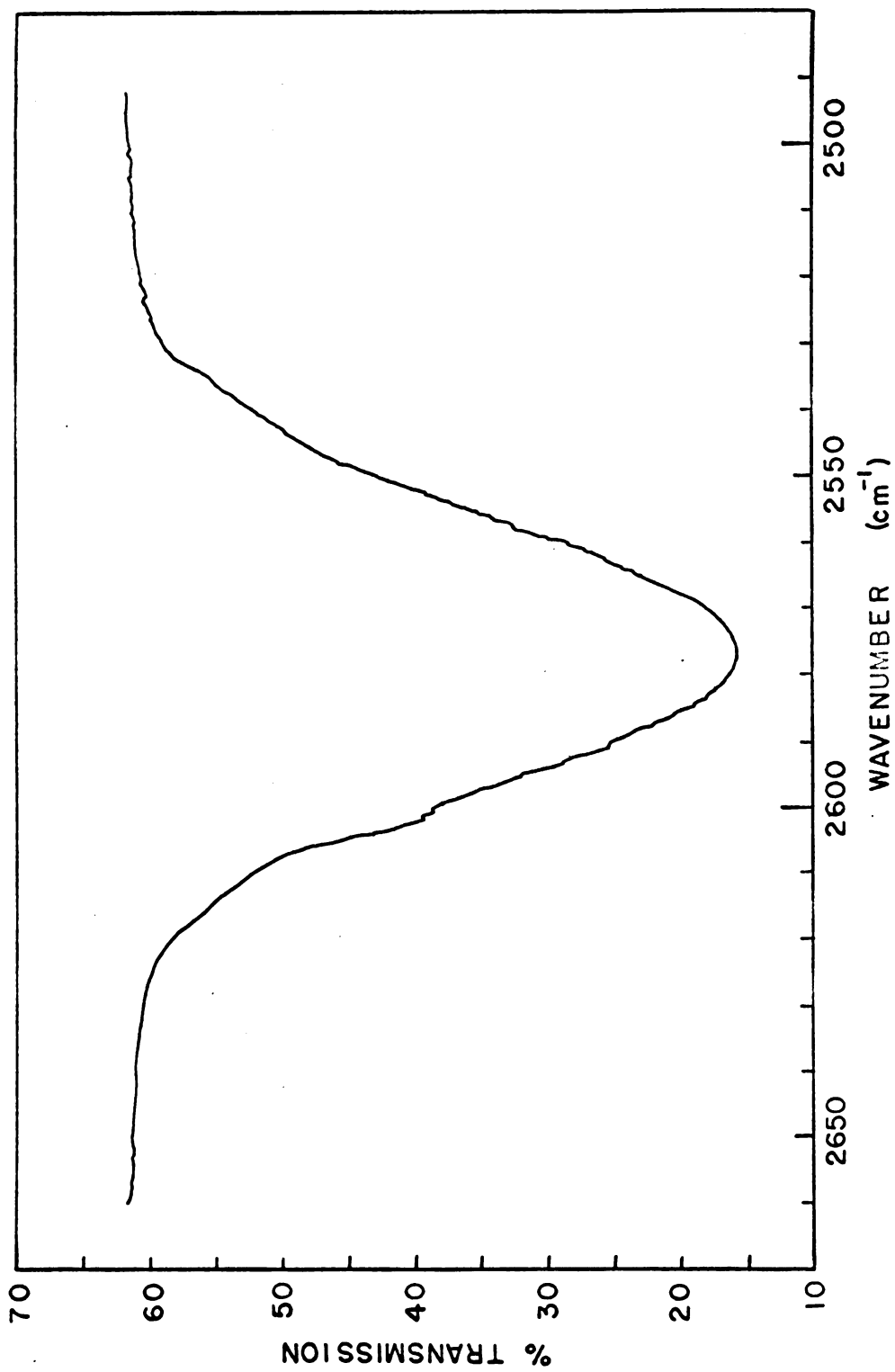


Fig. 16. - B-H terminal stretching band in decaborane vapor absorption spectrum.

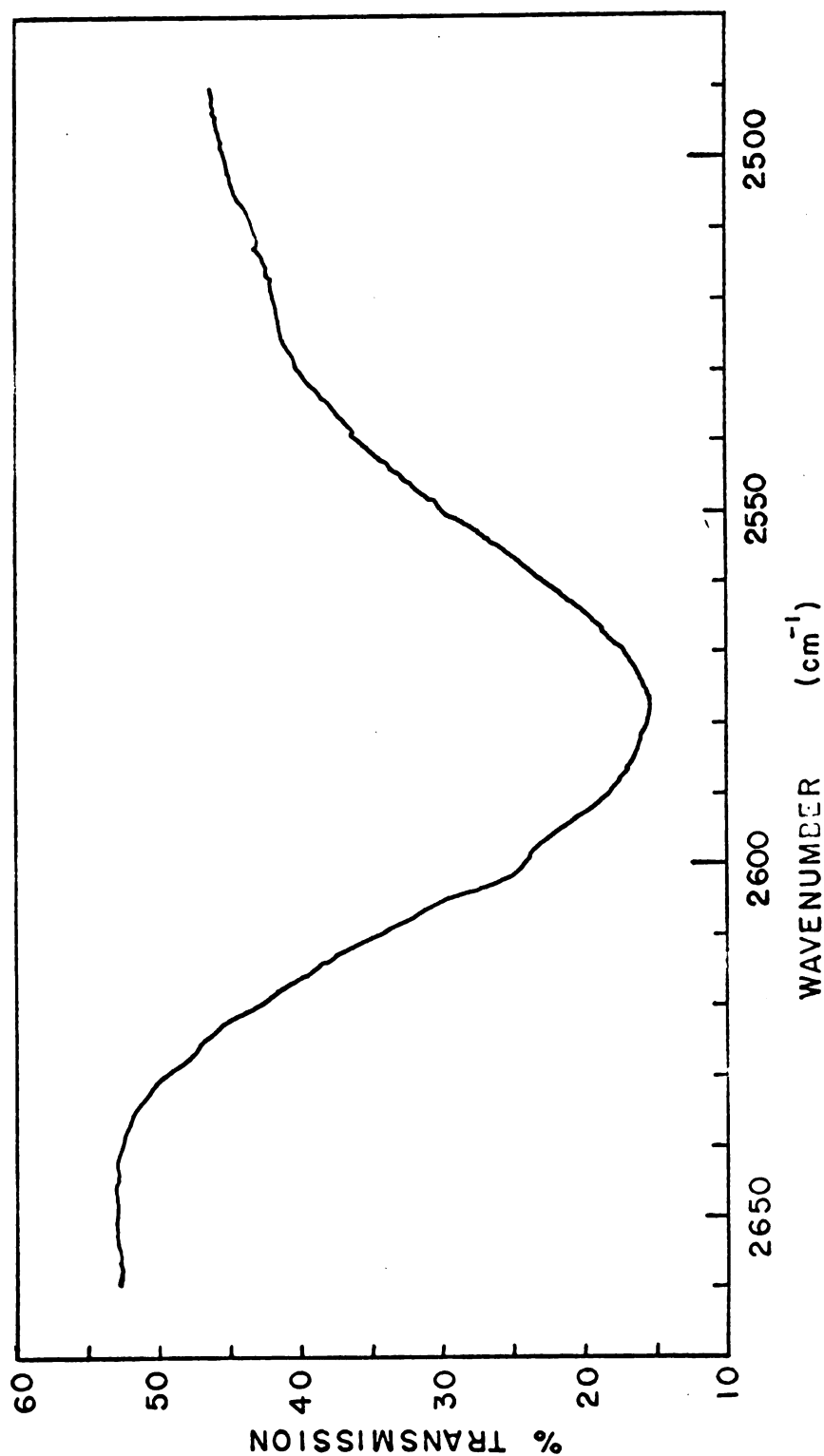


Fig. 17. - B-H terminal stretching band in decaborane solution (Nujol) absorption spectrum. The increase in transmission on the high-frequency side of the absorption is a result of the lack of balance between the absorption of the Nujol in the reference beam and in the sample beam.



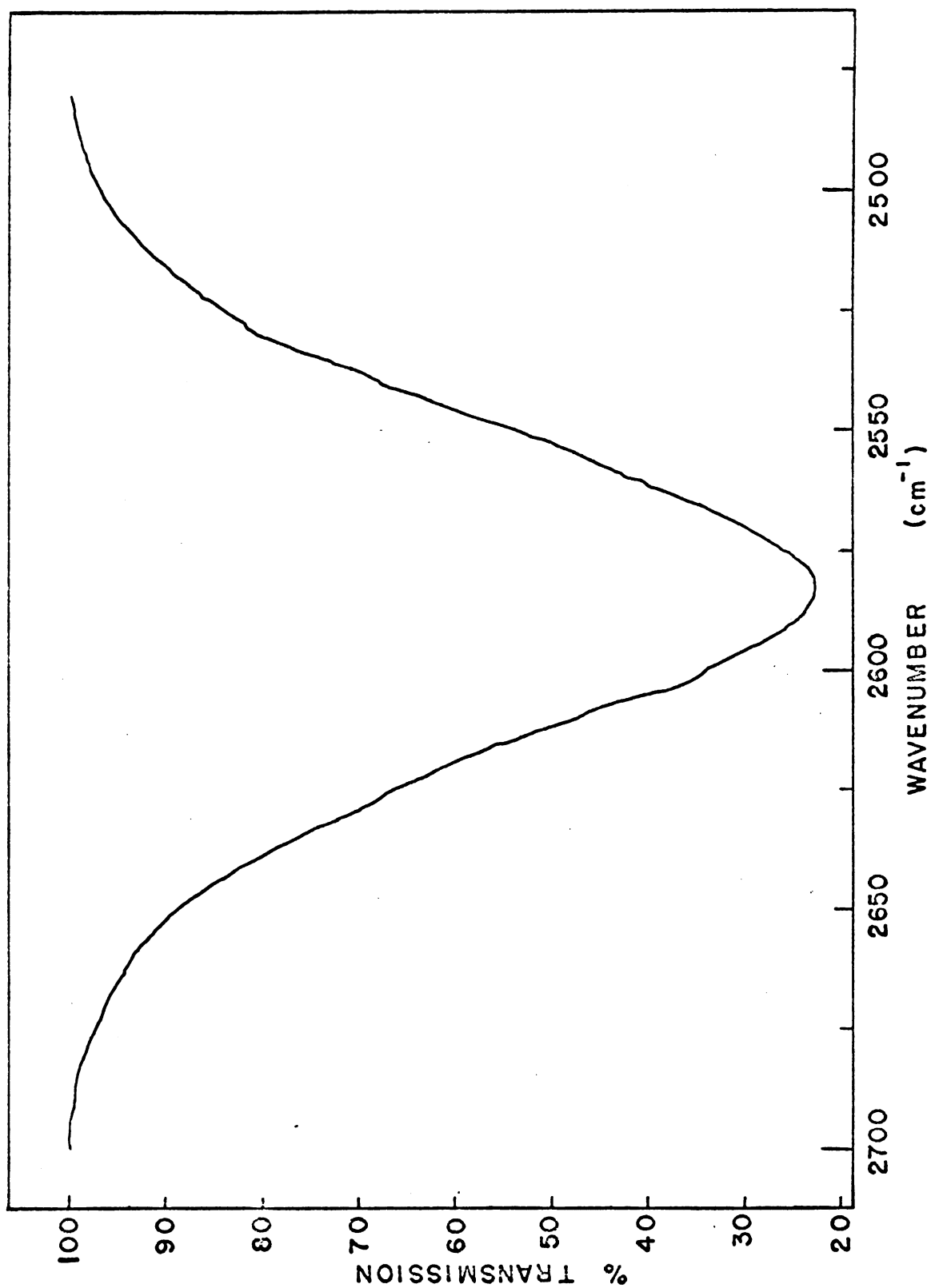


Fig. 18. - B-H terminal stretching band in decaborane solution (benzene) absorption spectrum.

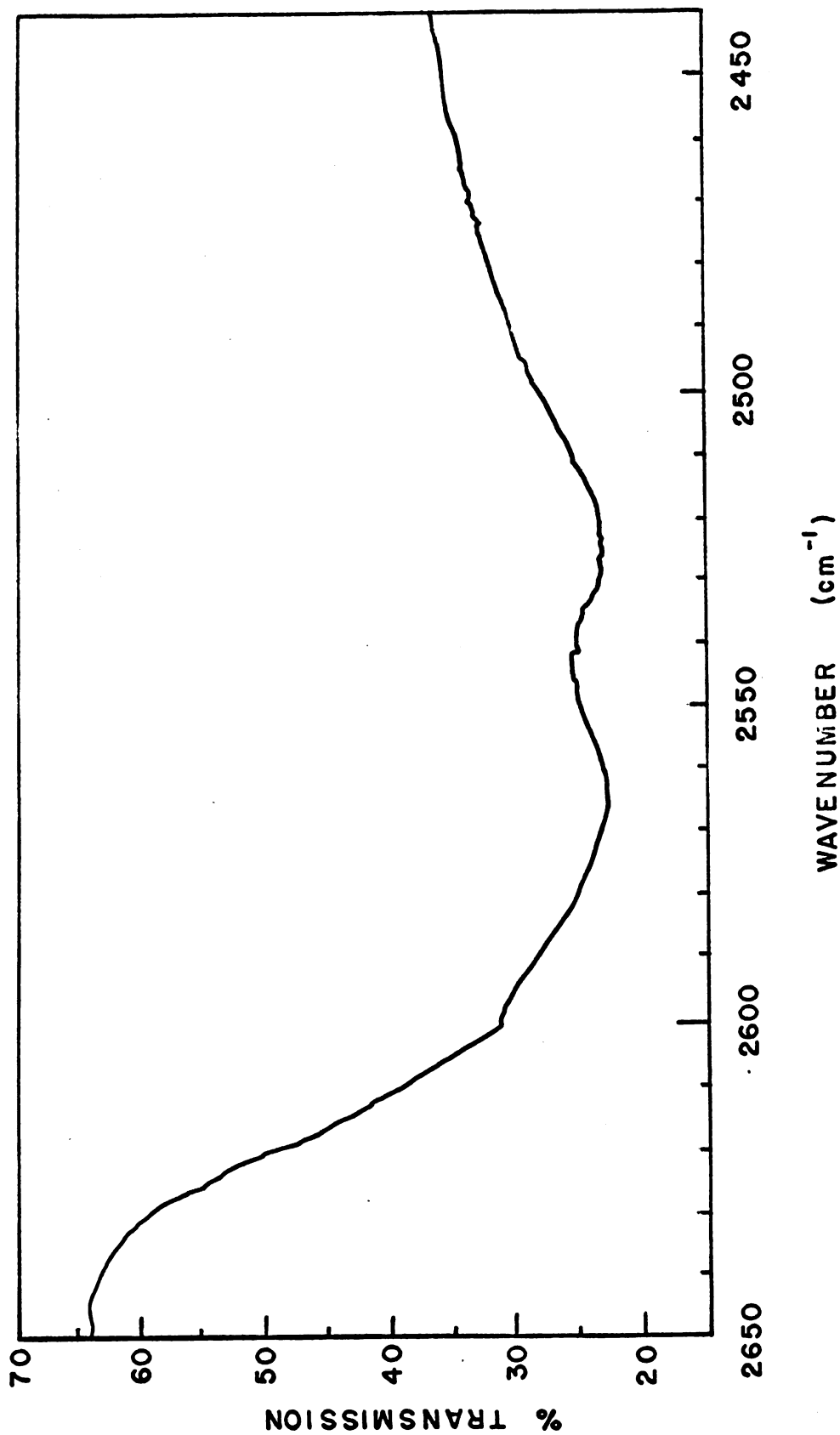


Fig. 19. - B-H terminal stretching band in decaborane pellet absorption spectrum. The large amount of transmission on the high-frequency side of the absorption is due to a Christiansen peak (See Section V, C - Christiansen Filter Effect).

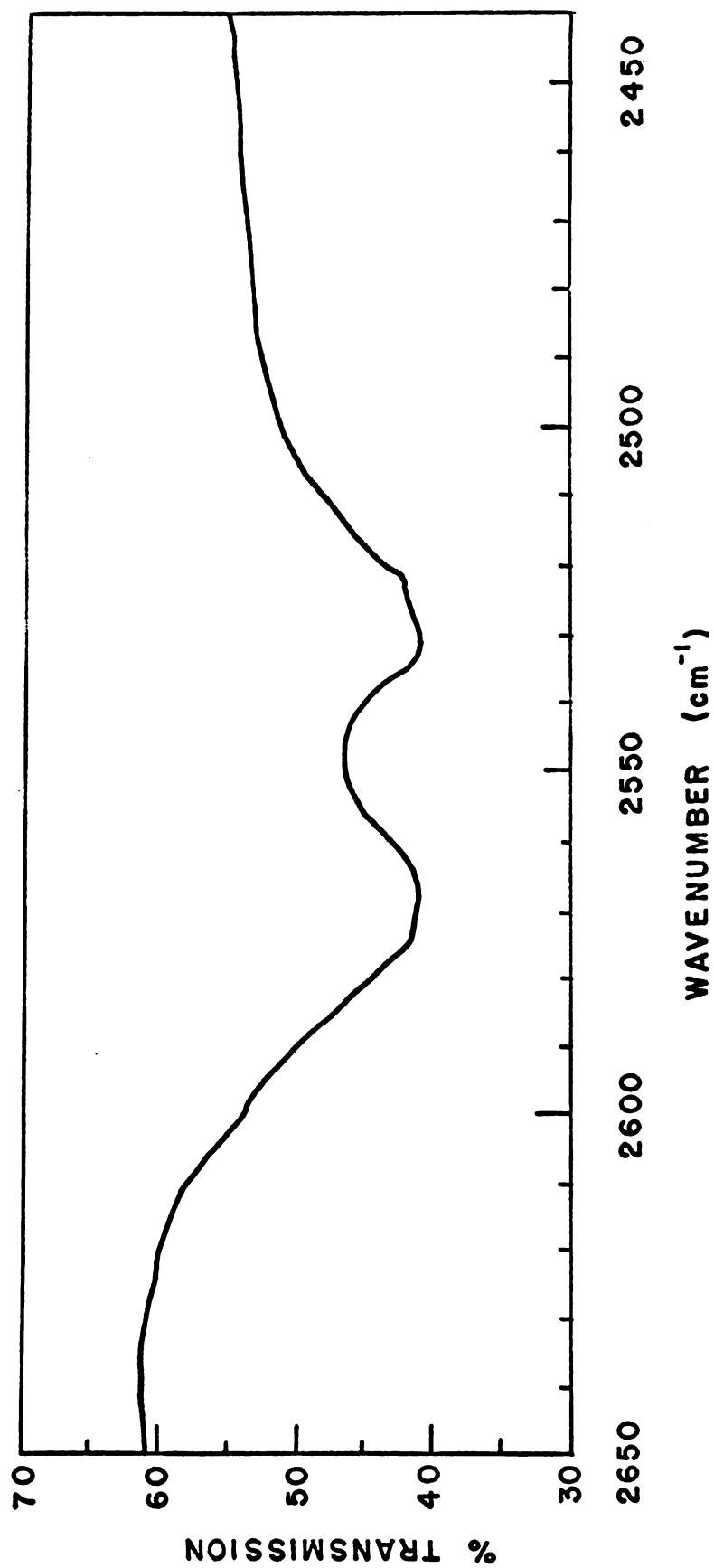


Fig. 20. - B-H terminal stretching band in decaborane film absorption spectrum.

TABLE II

B-H TERMINAL STRETCHING FREQUENCIES OF DECABORANE ( $\text{cm}^{-1}$ ).

<u>Scale</u>	<u>Vapor</u>	<u>Solution</u> <u>(Benzene)</u>	<u>Solution</u> <u>(Nujol)</u>	<u>Pellet</u>	<u>Film</u>
1 $\text{cm}/100 \text{ cm}^{-1}$	2587	2587	2575	2568 2528	2572 2531
10 $\text{cm}/100 \text{ cm}^{-1}$	2577	2583	2577	2564 2525	2569 2528
	2601	2601	2600	2601	2600

B-H terminal stretching mode:

- (a) The single absorption band in the vapor spectrum and in both solution spectra becomes a doublet in spectra for pellets and films.
- (b) The absorption frequency decreases slightly in going from the vapor and the solution to the solid.
- (c) The band width increases in going from the vapor to the solution to the solid (Fig. 21).

Meaningful intensity comparisons could not be made because different amounts of decaborane were contained in the specimens prepared by the various techniques.

### C. Christiansen Filter Effect

Curve a of Fig. 22 represents the dispersion curve for a crystal in the neighborhood of  $\lambda_0$ , the wavelength of the characteristic absorption. A suspension of small particles of this crystal in the transparent

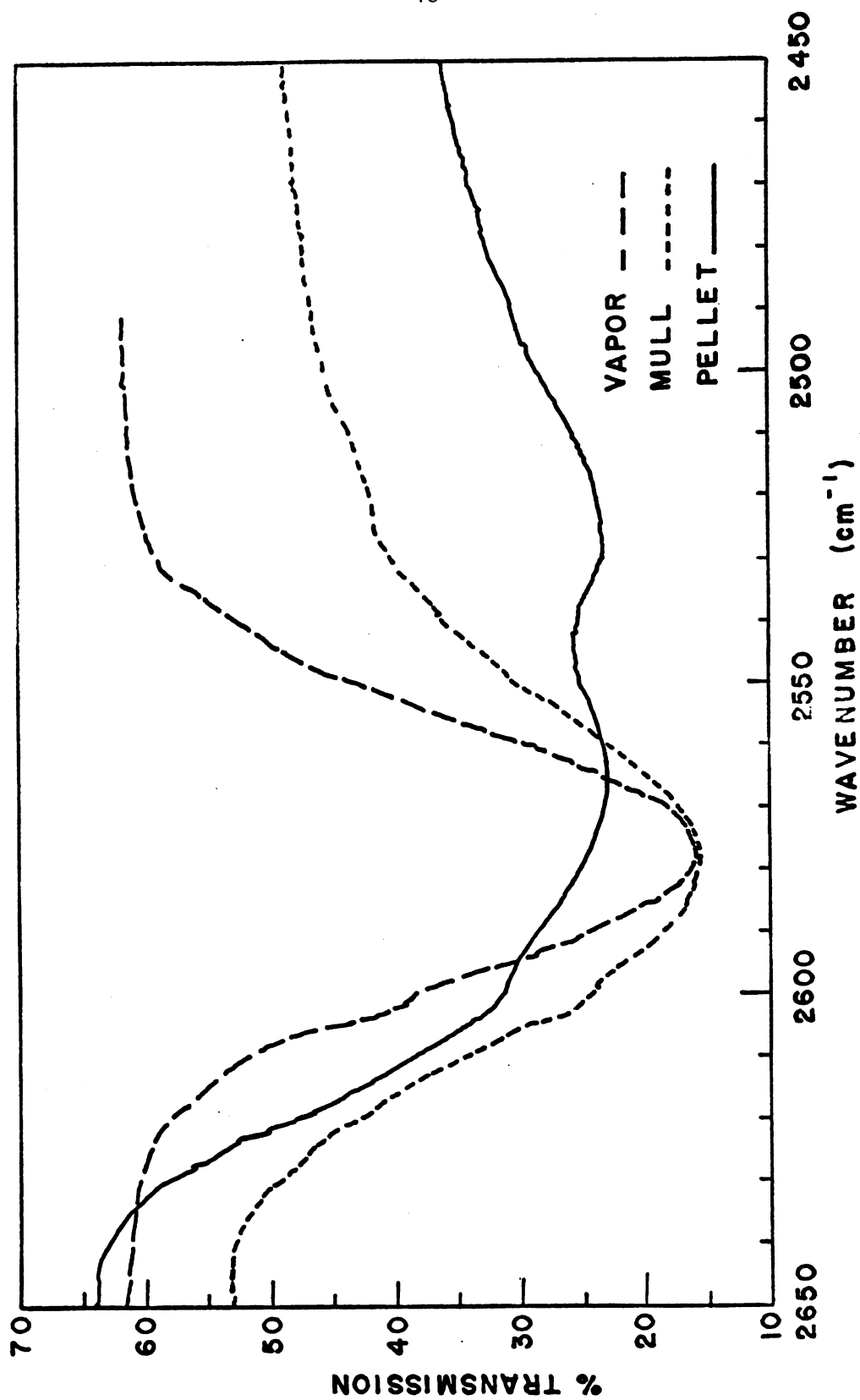


Fig. 21. - B-H terminal stretching band in vapor, solution, and pellet absorption spectra.

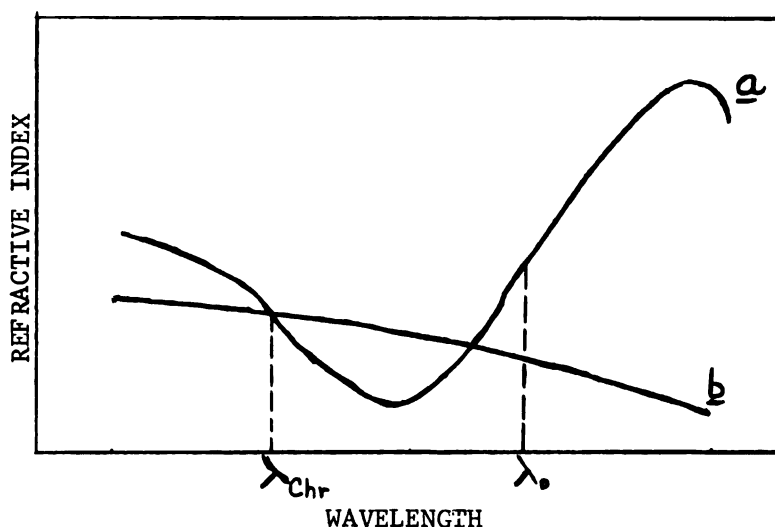


Fig. 22. - The dispersion curves for (a) a crystal in the neighborhood of characteristic absorption, and (b) a transparent medium.

medium whose dispersion curve is represented by curve b should show a maximum of transmission at the wavelength  $\lambda_{Chr}$  corresponding to the point of intersection of a and b. At this wavelength the sample is optically homogeneous, and light of this wavelength will be preferentially transmitted by the mixture, since it will not be scattered by the multiple refractions and reflections occurring at other wavelengths. The strong absorption in the region of  $\lambda_0$  masks another Christiansen peak which would otherwise occur at the second intersection of the two dispersion curves. The increase in transmission may also be observed at wavelengths far removed from the absorption band, as a result of the gradual crossing of the dispersion curves. The high transmission at  $\lambda_{Chr}$  is known as the Christiansen-filter effect, first observed by C. Christiansen<sup>24</sup> with visible light, and

later by Barnes and Bonner<sup>25</sup> in the infrared.

Abnormally high transmission peaks on the high-frequency side of the absorption bands appear in the  $B_{10}H_{14}$  pellet, vapor, and film spectra (Figs 5, 9, and 10). The most pronounced effect is in the pellet spectrum, as is to be expected, since the effect is greatest for particles of linear dimension slightly larger than  $\lambda_{Chr}$ .<sup>25</sup> The vapor spectrum shows an increase in transmission near the  $1509\text{ cm}^{-1}$  and  $860\text{ cm}^{-1}$  absorptions as well as at  $1200\text{ cm}^{-1}$ . Christiansen transmission should not appear in vapor spectra, since vapor particles are too small to act as refracting centers. The fact that the effect does appear in Fig. 9 indicates that crystals have deposited on the gas-cell windows during the scanning of the vapor (see Section IV, G - Vapor).

The B-H terminal-stretching absorption in the pellet and the vapor samples of  $B_{10}H_{14}$  are compared in Fig. 23 in order to show the difference in the transmission due to the Christiansen effect. The increase in transmission on the high-frequency side of the B-H stretching band is believed to be due to the equality of the refractive index of  $B_{10}H_{14}$  and KBr at  $2650\text{ cm}^{-1}$ . As an absorption band is approached from the low-frequency side, the refractive index increases until it reaches a maximum. This increase causes lower transmission owing to high reflectivity. The characteristic absorption only serves

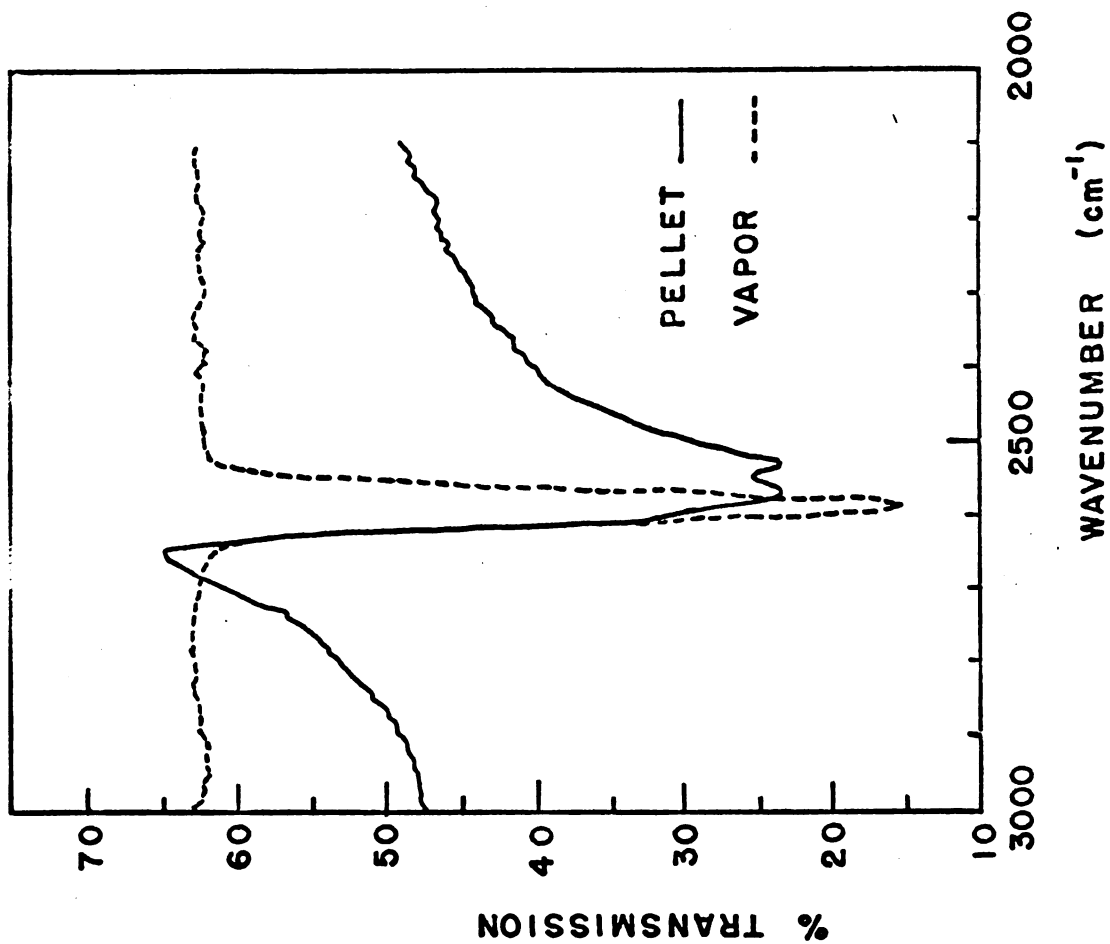


Fig. 23. - Decaborane pellet and decaborane vapor absorption spectra (B-H terminal stretching band).  
A Christiansen peak appears on the high-frequency side of the absorption in the pellet spectrum; no similar transmission peak is observed in the vapor spectrum.



to enhance the loss by multiple reflection and thereby further depress the transmission. This combined effect accounts for the slow decrease in transmission as the pellet absorption at  $2528\text{ cm}^{-1}$  is approached from lower frequencies.

## VI. INTERPRETATION OF RESULTS

### A. Crystal Structure

The crystal structure of decaborane was determined by Kasper, Lucht and Harker<sup>10</sup> in 1950. They described the structure as a partially-ordered system with a highly-twinned\* crystalline edifice at room temperature. To understand the partially-ordered lattice, we first consider the disordered structure and then the twinned, ordered structure.

Fig. 24a is a schematic diagram of the disordered structure projected on the (001) face. According to the notation of Kasper et al.<sup>10</sup>, a circle represents one-half the  $B_{10}H_{14}$  molecule, such as the half-molecule made-up of the primed borons and their bonded hydrogens shown in Fig. 1. Two circles and their connection represent one molecule; the direction of the connector between the circles is perpendicular to the  $B_V-B_{V'}$  bond. In the disordered structure\*\*, the

---

\*A twin may be defined as a crystal built up of two or more individuals of the same crystal species in intimate contact with each other over part of their bounding surfaces and oriented with respect to each other in certain well-defined ways. The components of a twin may be reflections of each other in a plane called the twinning plane. When there are two individuals, in contact along the twin symmetry plane, the crystal is called a contact twin. If individuals related in this way occur alternately and in large numbers, one has polysynthetic twinning. A high degree of polysynthetic twinning is found in the  $B_{10}H_{14}$  crystal structure. For a rather extensive treatment of twinning, the reader is referred to R. W. Cahn, *Advances in Physics* 3, 363 (1954).

\*\*This crystal system is orthorhombic and the space group is  $Pn\bar{m}$  ( $D_{2h}^{12}$ ) with parameters  $a_0 = 7.225\text{\AA}$ ,  $b_0 = 10.44\text{\AA}$ ,  $c_0 = 5.68\text{\AA}$ .

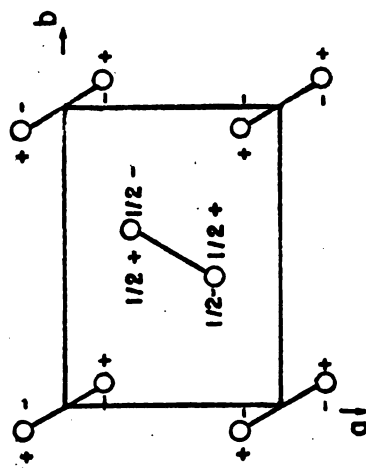


Fig. 24a. - Disordered crystal structure.

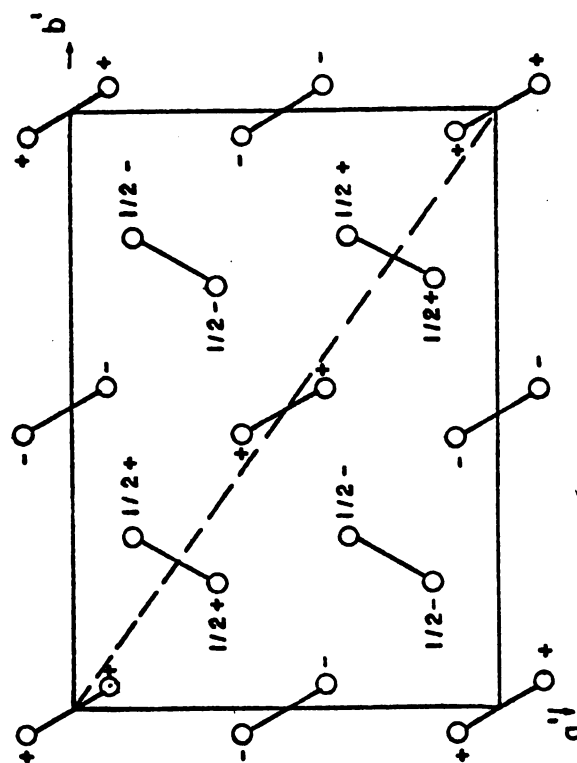
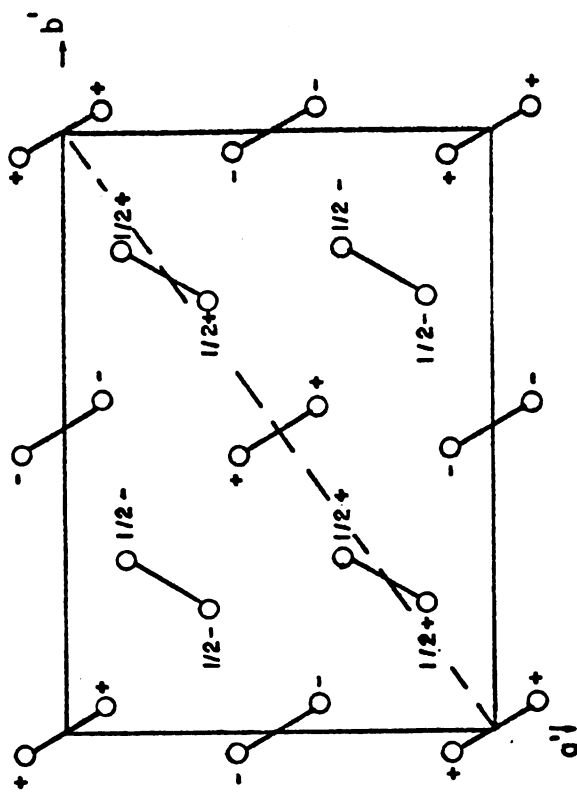


Fig. 24b. - Ordered crystal structure.

molecule occupies with equal probability either one set of orientations, or another set related to the first by a mirror plane parallel to the plane of the diagram. A plus or a minus next to a "half molecule" distinguishes between the two possible orientations; as it turns out in the actual structure, the two halves of every molecule are oriented in the same direction. Molecular models of the two orientations are shown in Figs 25 - 27. We arbitrarily assign a plus to the molecular orientation shown in Fig. 25, and assign a minus to the molecular orientation shown in Fig. 26. A plus and a minus appear with each circle in Fig. 24a because each orientation of the molecule is equally likely in the disordered state. The fraction  $\frac{1}{2}$  denotes that the plane of the half molecule is translated a distance  $c_0/2$  (2.84Å) in the  $\vec{c}^*$  direction from the plane of the other molecules. We choose to call the plane of the other molecules the base plane.

Fig. 24b is a schematic of the two ordered twins; that is, both twin A and twin B have ordered structures.\*\* The orientation of a

---

\*The vector  $\vec{c}$  is one of the three fundamental translation vectors (or primitive translation vectors) with the formal property that in the lattice, the atomic arrangement looks the same in every respect when viewed from any point  $\vec{r}$  as when viewed from the point  $\vec{r}' = \vec{r} + n_1\vec{a} + n_2\vec{b} + n_3\vec{c}$  where  $n_1, n_2, n_3$  are arbitrary integers.<sup>26</sup> In the case of the ordered structure due to the orthorhombic system,  $c$  is perpendicular to the plane of the diagram.

\*\*In both twins the crystal would be monoclinic and a monoclinic axes is indicated in the figure. The orthorhombic cell is used because of its relation to the small cell of the disordered crystal ( $a_0' = 2a_0$ ,  $b_0' = 2b_0$ ). The ordered space group is  $P2/c$  ( $C_{2h}^4$ ) with parameters  $a_0' = 14.45\text{\AA}$ ,  $b_0' = 20.88\text{\AA}$ ,  $c_0 = c_0' = 5.68\text{\AA}$ .

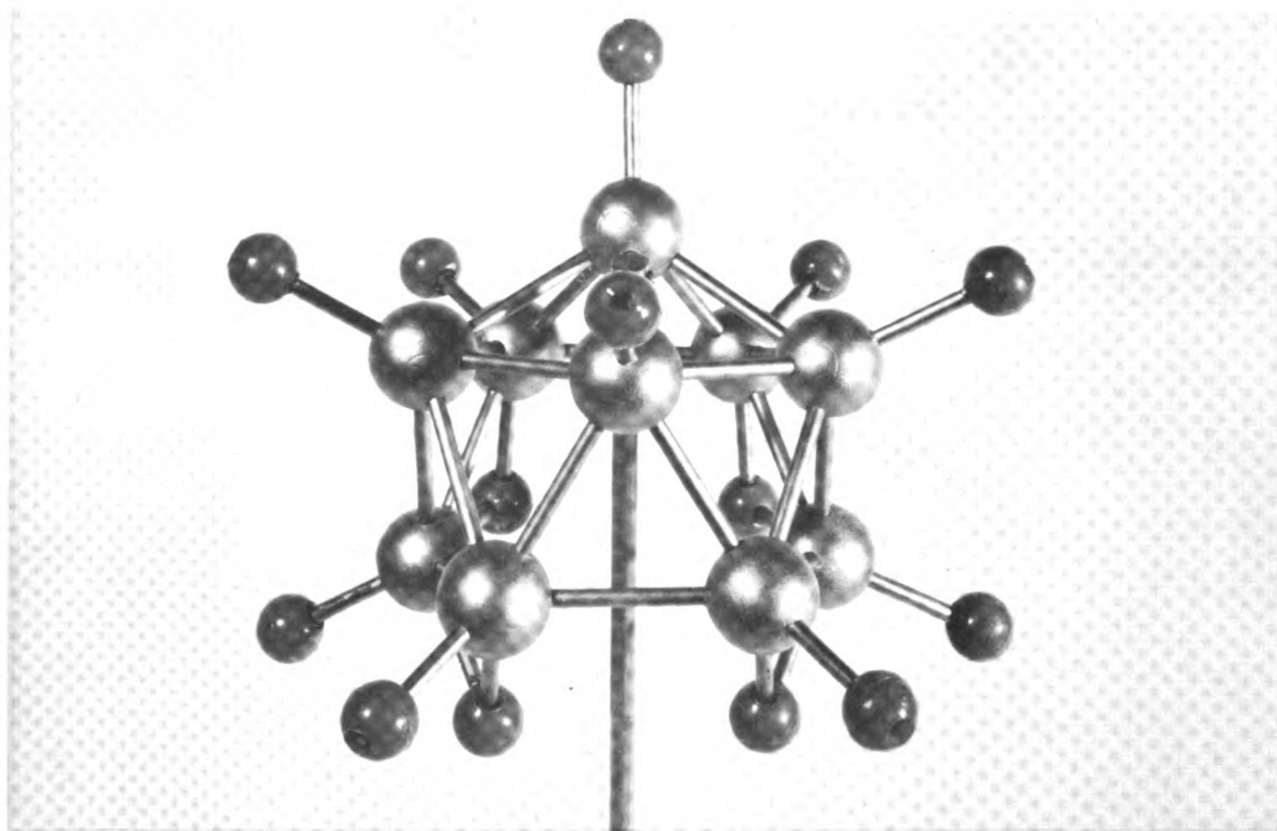


Fig. 25. - Model showing one of the two possible molecular orientations in the decaborane crystal lattice. This particular orientation is specified by a plus in Fig. 24.

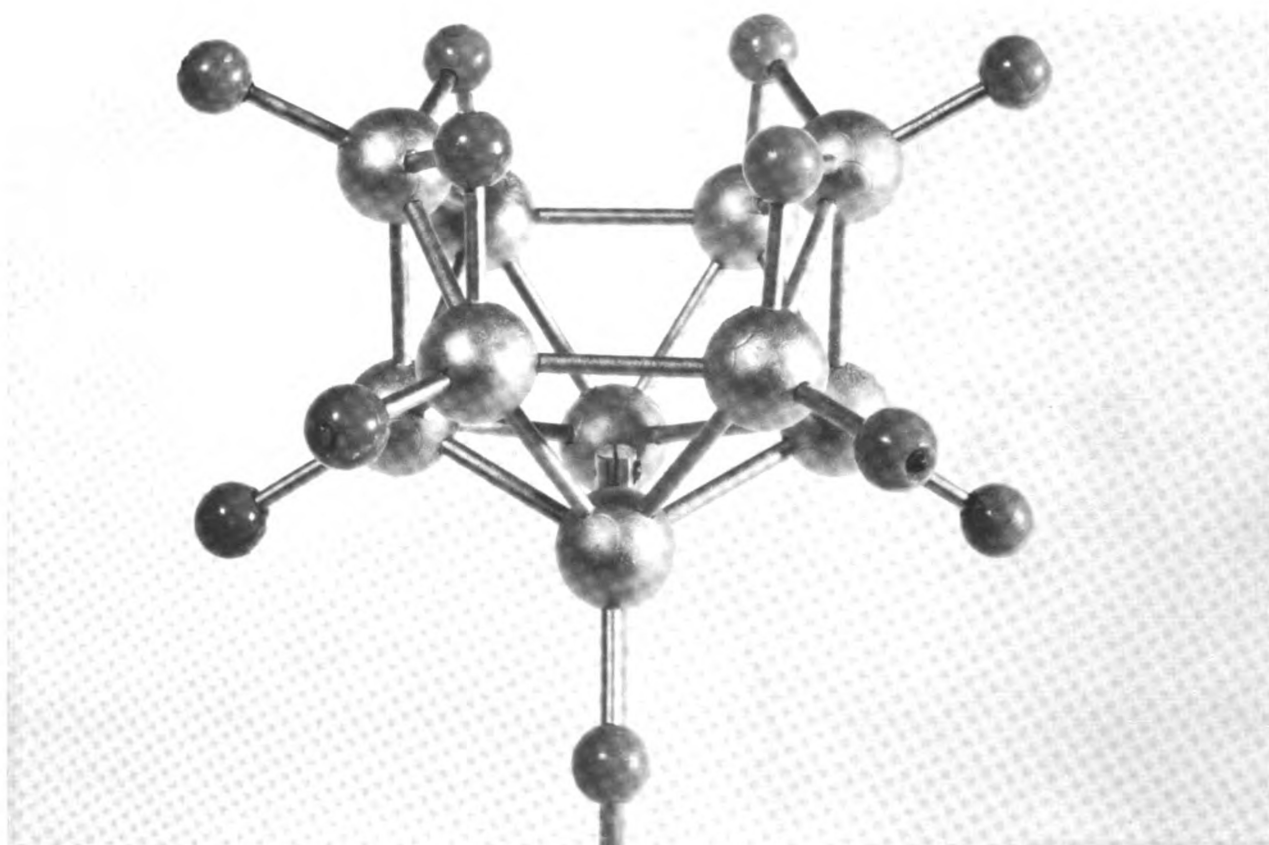


Fig. 26. - Model showing one of the two possible molecular orientations in the decaborane crystal lattice. This particular orientation is specified by a minus in Fig. 24. Three hydrogen atoms are not observable from this view, but appear in Fig. 27.

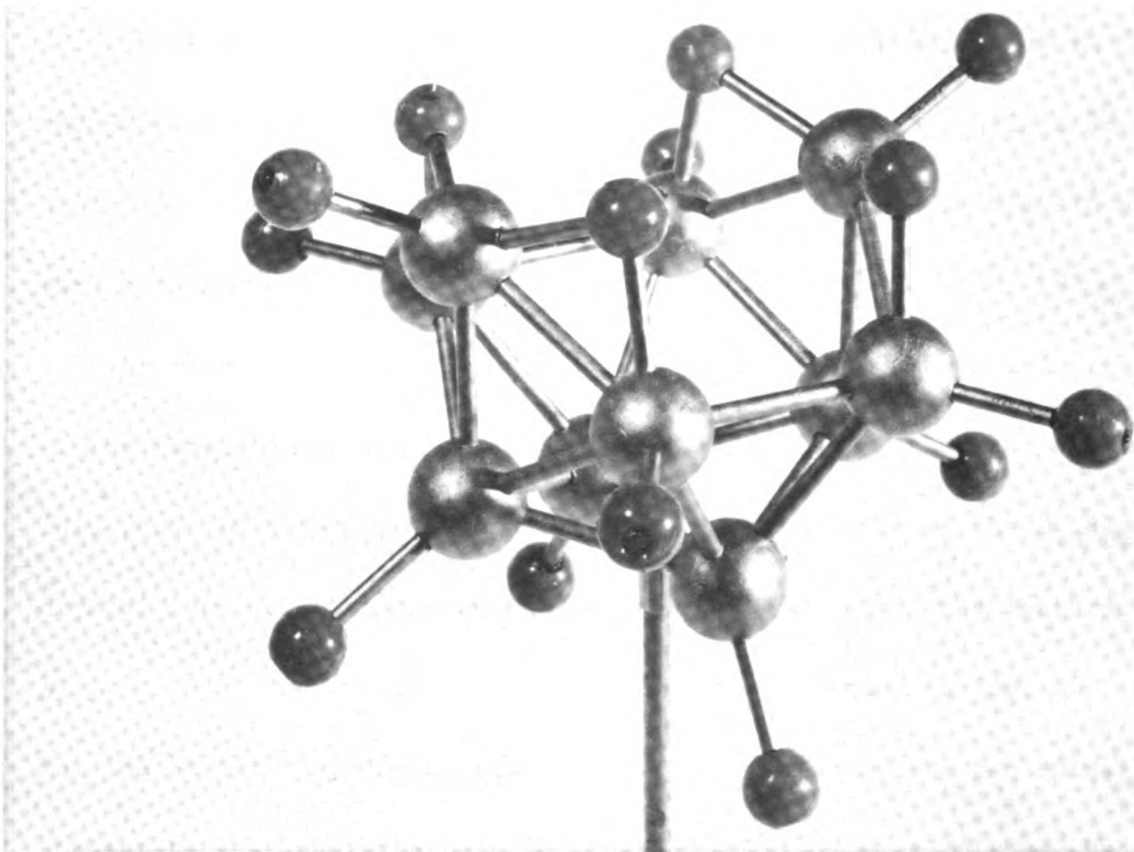


Fig. 27. - Model shown in Fig. 26, except that all 14 hydrogen atoms and all 10 boron atoms can be seen.

molecule is denoted by the plus-minus notation applied to the disordered structure. In the ordered system, however, each molecule may be in either one orientation or the other, but not in both. Twin A and twin B differ only in the orientation of the four molecules in the plane translated a distance  $c_0/2$  from the base plane. Figs 28 - 30 show models of the twinned structures. Twin A is shown in Fig. 28 and twin B is shown in Fig. 29.

At room temperature there exists a variation in the periodicity of the molecular orientation along the b direction of the lattice. This periodic structure is the partially-ordered state of the  $B_{10}H_{14}$  crystal lattice. Suppose we consider twin A and assign the letters a, b, c, d to the xz-layers of the structure, as shown in Fig. 31. For the partially-ordered state, there is a mixing of the two twins subject to the condition that an a or b layer is always followed by only a c or a d layer. It was assumed by Kasper that the four layers (a, b, c, d) occur with equal frequency, and that correlation exists between neighboring layers only by the condition that a or b is always followed only by c or d. A possible grouping of xz-layers in the partially-ordered structure is as follows:

...acbdacbd...acbdadbcadbc...adbcbcad...

The probability that a specific layer has the same kind of layer as a second neighbor was found<sup>10</sup> to be 1/20.



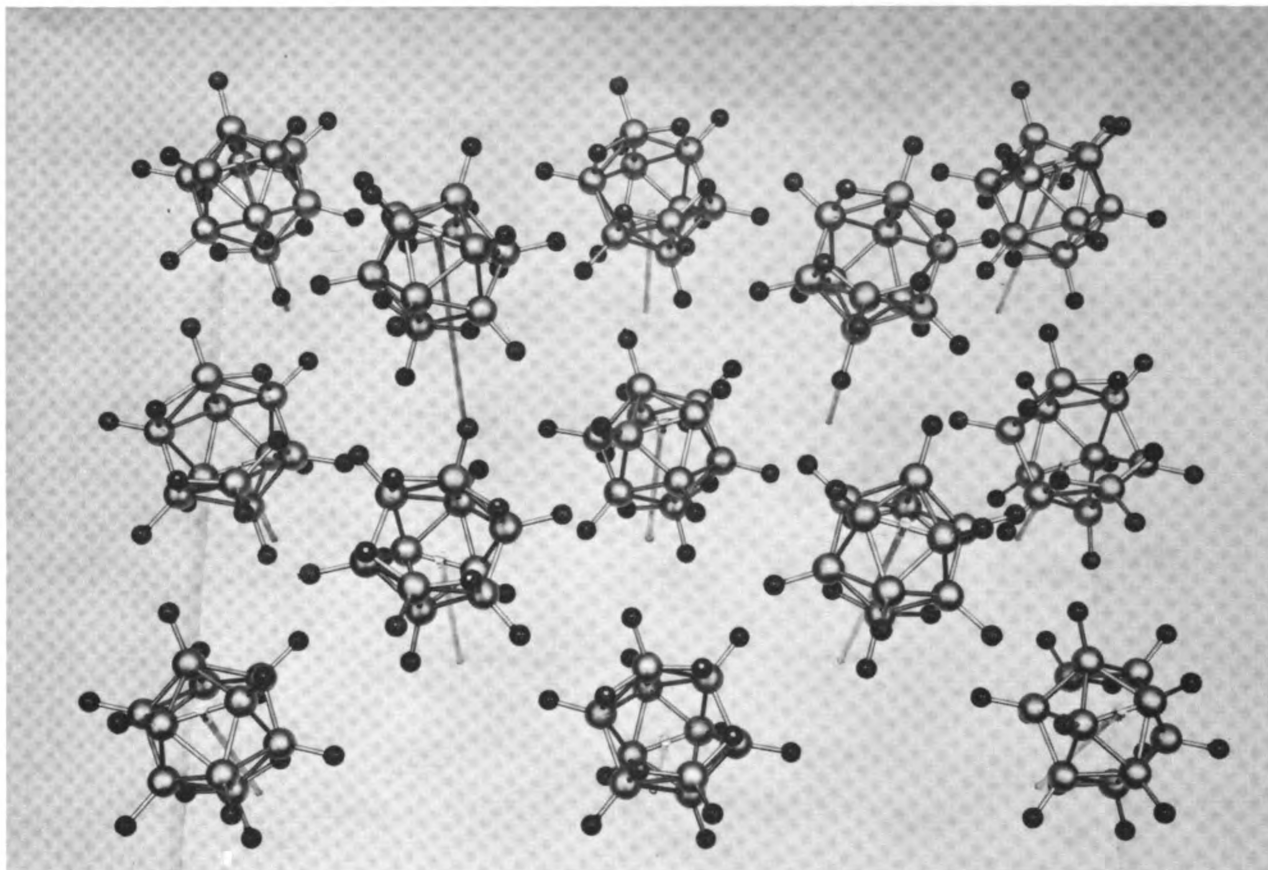


Fig. 28. - Decaborane ordered crystal structure--twin A.

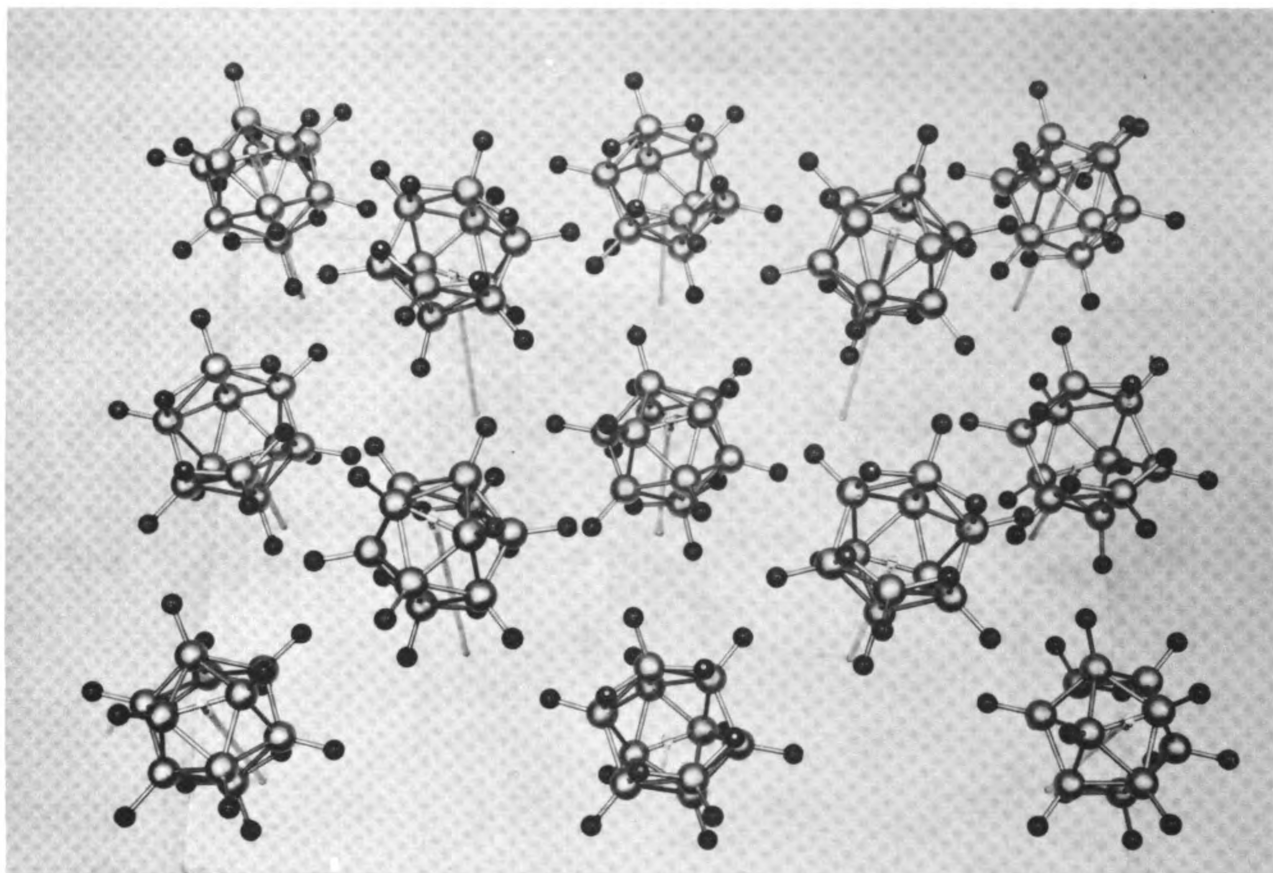


Fig. 29. - Decaborane ordered crystal structure--twin B.

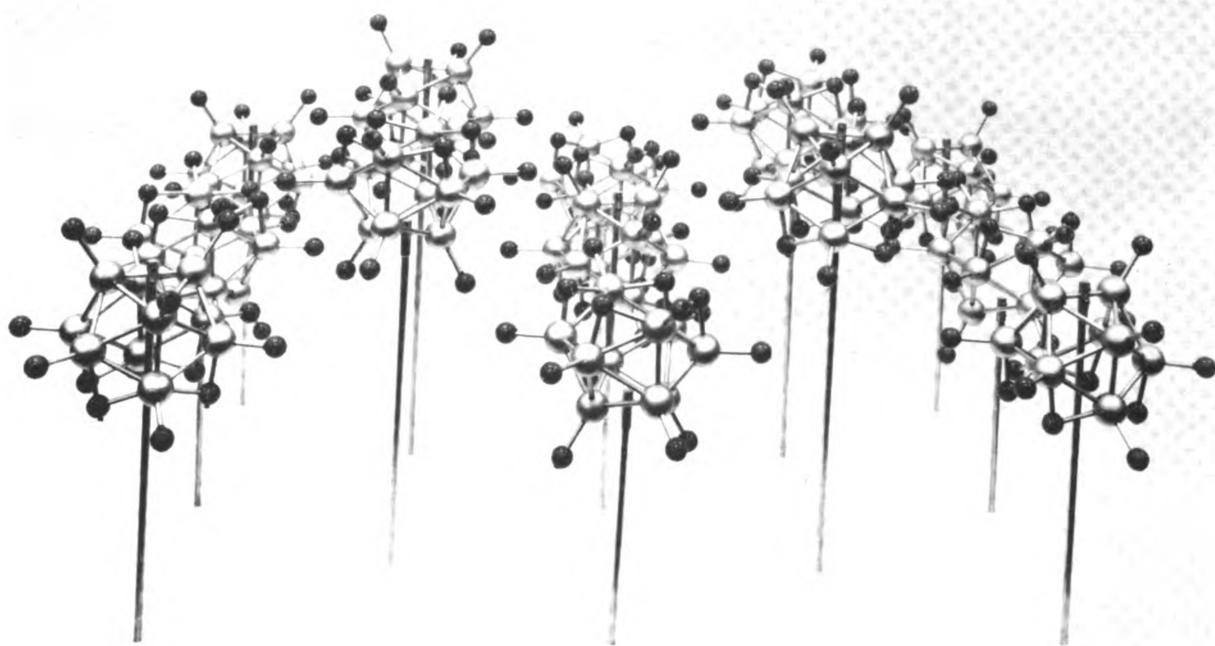


Fig. 30. - View of twin A showing the relative distance between the base plane molecules and the molecules in the plane translated in distance  $c_0/2$  from the base plane (also observed in twin B).

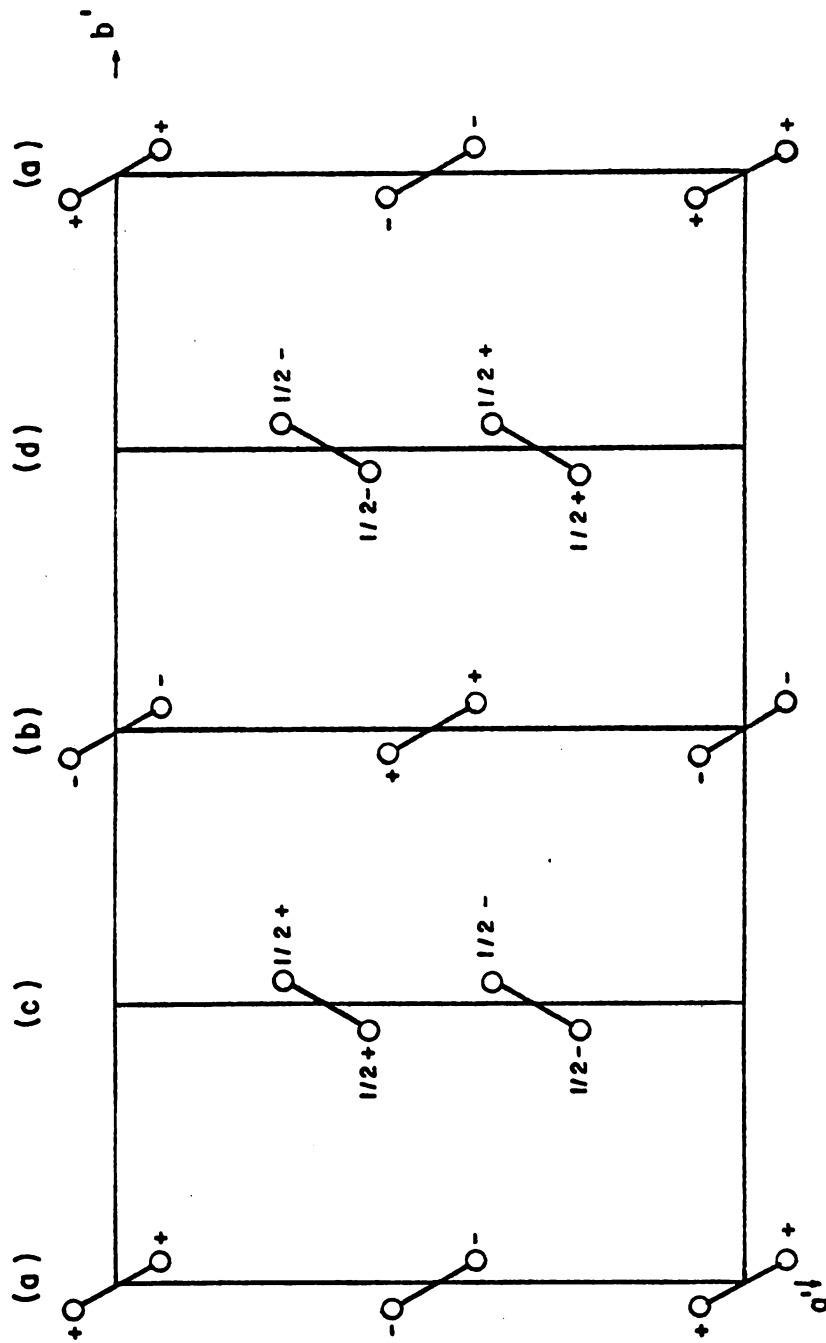
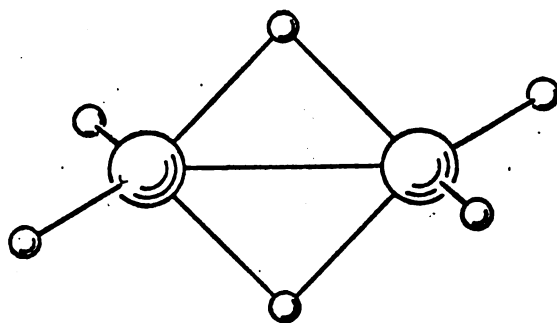


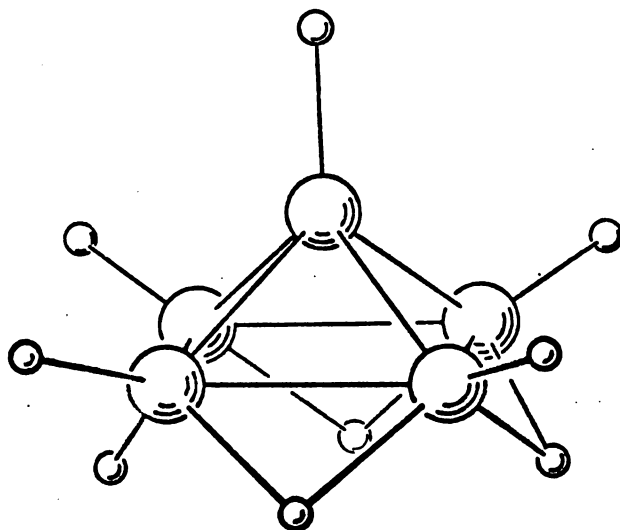
Fig. 31. - Schematic diagram illustrating the arrangement of xz-layers for twin A.

## B. Origin of Spectra Variations

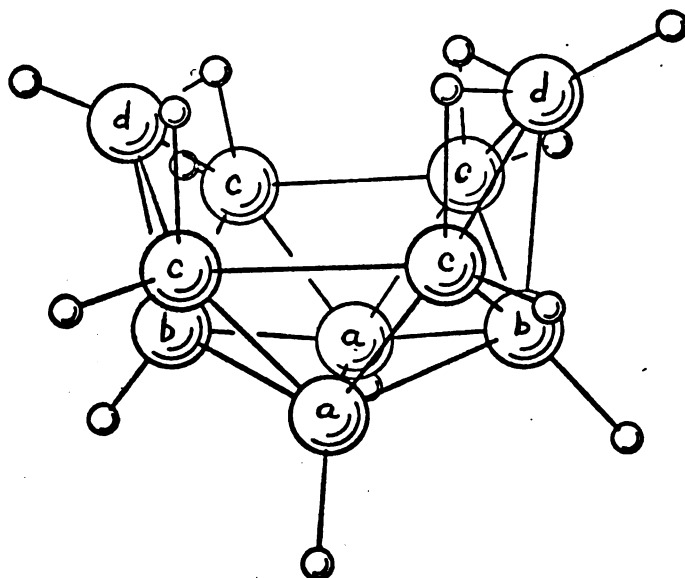
We are now in a position to describe accurately what are considered to be the origins of the observed bands. Let us first consider the spectrum of the molecule alone as it appears in the vapor. The band that has been the center of our interest, near  $2600\text{ cm}^{-1}$ , is attributed to the 10 terminal hydrogens, each stretching the single bond connecting it to a single boron atom. The basis of this assignment is that in general a hydrogen atom bonded to a heavier atom vibrates with a high frequency (cf. C-H,  $3000\text{ cm}^{-1}$ ; N-H,  $3300\text{ cm}^{-1}$ ; O-H,  $3600\text{ cm}^{-1}$ ), and specifically that B-H stretching vibrations in diborane (Fig. 32a) and pentaborane (Fig. 32b) have frequencies in the region  $2500 - 2600\text{ cm}^{-1}$ . Moreover, the large change in dipole moment occurring in this mode, and the large number of terminal atoms, point to a strong absorption, as is indeed observed. The 10 terminal hydrogen atoms are not all equivalent, however, so some structure might be expected in the band. We believe that the shoulder at  $2600\text{-}2601\text{ cm}^{-1}$  reflects this non-equivalence. As shown in Fig. 32c, the hydrogen atoms attached to boron atoms V and V' form a set of equivalent atoms (labeled a), those attached to II and II' another set of equivalent atoms (labeled b), those attached to I, IV, I', IV' another set of equivalent atoms (labeled c), and those attached to III and III' still another (labeled d). We ascribe, for reasons discussed later, the shoulder to the group of equivalent B-H atoms



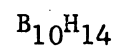
(a) diborane



(b) pentaborane



(c) decaborane



(The four sets of  
B-H pairs are  
labeled a,b,c,d.)

Fig. 32. - (From L. Pauling, The Nature of the Chemical Bond)

labeled a. Strictly speaking, of course, we should talk only about normal vibrations, in which all atoms participate. But the high frequency of this band results in almost no coupling with the lower frequencies of other vibrational modes of the molecule. Hence it makes sense to speak about stretching vibrations of hydrogen atoms alone.

The next mode to be considered is that of the stretching of the four bridged hydrogen atoms. Because of the bridged nature of the bond, stronger bonds might be expected; the inter-atomic distances, however, are 1.34 - 1.40 Å compared to 1.25 - 1.29 Å for the terminal-hydrogen bonds indicating a weaker bridged-hydrogen bond. Hence a priori, it is difficult to say where the absorption should lie. In early studies with pentaborane Hrostowski and Pimentel<sup>21</sup> ascribed bands in the 1800 - 2140  $\text{cm}^{-1}$  region to B-H bridge stretching vibrations. But Shapiro, Wilson, and Lehman<sup>23</sup> found that bands in this region for diborane ( $\text{B}_2\text{H}_6$ ) disappeared when one terminal hydrogen was replaced by an alkyl group ( $\text{CH}_3$  or  $\text{C}_2\text{H}_5$ ), but reappeared when two terminal hydrogens were replaced by alkyl groups. Hence absorption in this region appears to be connected with vibrations of terminal rather than bridged hydrogens. Shapiro et al. definitely assign a band at 1500  $\text{cm}^{-1}$  to the bridge-stretching mode in the alkyl diboranes, but warn that the frequency of this mode is dependent upon the parent boron hydride.

Modes representing deformation of the skeleton would be expected to lie farther out in the infrared; indeed, the complex absorption pattern appearing around  $1000\text{ cm}^{-1}$  is attributed to B-B skeletal stretching, and that around  $300\text{ cm}^{-1}$  to skeletal bending.<sup>13</sup> Important as these bands are, they are so complex that their study is best left as a separate study.

In the dilute solutions studied, the band near  $2600\text{ cm}^{-1}$  appeared to broaden somewhat. Such an effect is expected. In substances where a strong rotational broadening of the vibrational lines occurs in the vapor phase, the quenching of the rotation in solution will tend to narrow the lines. But the difference in environment from one decaborane molecule to another in the solution will widen the vibrational lines.<sup>27</sup> In decaborane, rotational broadening should be slight because of its symmetrical structure, but environmental broadening should be appreciable.

In the solid, the effect of interaction of the terminal hydrogens with neighbors on adjacent molecules appears strong. The line does not merely broaden, but actually appears as a doublet, the shoulder on the high-wavenumber side persisting. There is a slight decrease in the frequency of the minima of the doublet as compared with that of the minimum of the single band of the vapor and solution. The decrease in frequency may be made plausible in the following way. If molecules in the condensed phase attract each other, the electronic configuration



of the molecule is so modified as to give weaker bonding within the individual molecule than exists between the atoms of the molecule in the condensed phase.<sup>27</sup> In other words, by building the molecules into a crystal lattice, associative bonds are formed between atoms of neighboring molecules; the original valency bonds within the molecule are subsequently weakened so that the frequency of the intra-molecular vibrations are decreased.<sup>17</sup>

We attribute the origin of the doublet to different sets of terminal hydrogen atoms as they are positioned with respect to their neighbors in the lattice. That is, since a shoulder and single absorption band appear in the vapor and solution spectra, we explain the shoulder plus the doublet in the solid spectrum in terms of the inter-molecular environment in the decaborane crystal. Consideration of the crystal structure (Fig.s 28 - 30) shows that the set of terminal hydrogen atoms labeled d in Fig. 32c, has essentially the same atomic environment as the set of hydrogen atoms labeled b.\* We consequently assign the minimum of the doublet appearing near  $2525\text{ cm}^{-1}$  to the bond stretching of the B-H pairs indicated by the set of hydrogen atoms labeled b and by the set labeled d. The hydrogen atoms of set a have a nearest-neighbor environment consisting of a single atom of the c

---

\*An atom of the d set has a nearest-neighbor environment consisting of two atoms of the c set and an atom of the b set; an atom of the b set has an environment of two atoms of the c set and an atom of the d set.

set. We assume that the condensed environment of the lattice has a negligible effect on the B-H stretching vibrations involving the hydrogen atoms of set a. We assign the shoulder exhibited in all spectra near  $2600\text{ cm}^{-1}$  to this set. The minimum of the doublet appearing near  $2565\text{ cm}^{-1}$  is attributed to the stretching vibrations of the hydrogen atoms of set c. Obviously, this set has a nearest-neighbor environment consisting of hydrogen atoms of the d set or of the b and of the a sets.\*

### C. Analysis of Line Shape

No rigorous theoretical expression has been derived for the line shape in an absorption spectrum. For many purposes, a linear damped harmonic oscillator is taken as the basis of an ad hoc representation. This analysis, both for isolated molecules<sup>28</sup> and for ionic solids,<sup>1</sup> leads to the following expression for the complex dielectric constant  $\epsilon$  as a function of angular frequency  $\omega$ :

$$\frac{\epsilon(\omega) - \epsilon(\infty)}{\epsilon(0) - \epsilon(\infty)} = \frac{1}{1 - (\omega/\omega_0)^2 - i(\omega/\omega_0)(\gamma/\omega_0)}$$

Here  $\epsilon(0) \equiv \epsilon_0$ , the static dielectric constant, is the limiting value of  $\epsilon$  as  $\omega$  approaches zero;  $\epsilon(\infty) \equiv \epsilon_\infty$ , the high-frequency dielectric constant, is the limiting value at frequencies high enough that ion-core

---

\*All of the discussions concerning the environment of the hydrogen atoms are independent of both molecular orientation and the plane of the molecule in the unit cell.

motion has ceased, but not so high that electronic transitions occur.

The parameter  $\omega_0$ , the infrared-dispersion frequency, is a kind of resonance frequency; the parameter  $\gamma$ , the damping constant, is related to the half-width of the absorption peak.

For optical studies, we need the complex refractive index  $\bar{n}$ , defined as

$$\bar{n} \equiv (\epsilon \mu)^{1/2} \equiv n + ik$$

where  $\mu$ , the magnetic permeability may be taken as unity for nonmagnetic substances. Here  $n$  is the ordinary (real) refractive index, and  $k$  is an absorption coefficient. It is easy to show that

$$n^2 - k^2 = \epsilon_\infty + \frac{(\epsilon_0 - \epsilon_\infty)[1 - (\omega/\omega_0)^2]}{[1 - (\omega/\omega_0)^2]^2 + (\omega/\omega_0)^2(\gamma/\omega_0)^2} \equiv A^2$$

and

$$2nk = \frac{(\epsilon_0 - \epsilon_\infty)(\gamma/\omega_0)(\omega/\omega_0)}{[1 - (\omega/\omega_0)^2]^2 + (\omega/\omega_0)^2(\gamma/\omega_0)^2} \equiv B^2.$$

Standard electromagnetic theory is then applied as is appropriate to the specific experimental situation.

Each component of a plane electromagnetic wave, traveling in the direction of the positive  $z$ -axis, is proportional to

$$\begin{aligned} e^{2\pi i(\mathcal{D}z - \nu t)} &= e^{2\pi i \nu / \bar{\lambda} z / c} e^{-2\pi i \nu t} \\ &= e^{2\pi i \nu (\pi z / c)} e^{-2\pi k \nu z / c} e^{-2\pi i \nu t}, \end{aligned}$$

where  $\bar{\nu} = 1/\lambda = \nu/c$ ,  $\lambda$  being the wavelength in vacuo, and  $c$  the speed of light. The intensity  $I$  is proportional to the square of the absolute value of the amplitude, that is,

$$e^{-4\pi k z/c} = e^{-2\omega k z/c} = e^{-2k \cdot 2\pi z/\lambda}$$

1. Absorption by Thin Films. By standard theory, the transmission coefficient  $T = I/I_0$  for electromagnetic radiation of wavelength  $\lambda = 2\pi c/\omega$  incident normally on a plane parallel plate of thickness  $d$  is given by

$$1/T = \left| [(1 + \bar{n})^2 e^{-i\pi 2\pi d/\lambda} - (1 - \bar{n})^2 e^{i\pi 2\pi d/\lambda}] / 4\bar{n} e^{-i2\pi d/\lambda} \right|^2.$$

When the value for  $\bar{n} = \epsilon^{\frac{1}{2}}$  is substituted in this equation, the resulting equation is awkward to solve for  $\omega_0$  and  $\gamma$ . As shown in Montgomery and Yeung,<sup>29</sup> a good approximation is provided by

$$\begin{aligned} 1/T \cong & 1 + (2nk)(2\pi d/\lambda) \\ & + \left\{ [(n^2 + k^2)^2 - 2(n^2 - k^2) + 1] / 4(2nk)^2 \right\} (2nk)^2 (2\pi d/\lambda)^2 \\ & + \left\{ 1/3 [1 - (n^2 - k^2)] / (2nk)^2 \right\} (2nk)^3 (2\pi d/\lambda)^3 + \dots \end{aligned}$$

For transmission from 100% to about 25%, the terms in  $d^3$  and higher may be neglected; and in the neighborhood of the absorption peak, as explained in Montgomery and Yeung, the coefficient of the term in  $d^2$  simplifies, and we may write

$$\frac{1}{T} - 1 \cong \frac{(\epsilon_0 - \epsilon_\infty)(2\pi d/\lambda) \{ 1 + \frac{1}{2} [(\epsilon_0 - \epsilon_\infty)/(\gamma/\omega_0)] (2\pi d/\lambda_0) \}}{(\omega/\omega_0 - \omega_0/\omega)^2 + (\gamma/\omega_0)^2}$$

We see that  $T^{-1} - 1$ , and hence  $T$ , is symmetric in  $\omega/\omega_0 = \bar{\nu}/\bar{\nu}_0 = \lambda/\lambda_0$

and its reciprocal. Hence there are two values of  $\bar{\nu}$  (labeled  $\bar{\nu}_+$  and  $\bar{\nu}_-$ ) for a given value of  $T$ . It follows immediately that

$$\bar{\nu}_0 = (\bar{\nu}_+ \bar{\nu}_-)^{\frac{1}{2}}$$

A plot of  $(\bar{\nu}_+ \bar{\nu}_-)^{\frac{1}{2}}$  against  $T$  should give a horizontal line at ordinate

$\bar{\nu}_0$  over the domain of the abscissa  $T_{\min} \leq T \leq T_{\infty}$ . The success of this technique has been discussed by Montgomery and Yeung, loc. cit. for their work with lithium fluoride and lithium hydride, where considerable success has been achieved. In the present work, however, the principle absorption peak splits into a doublet. Hence this analysis cannot be applied directly. Modifications of it are possible, but we have not yet been able to demonstrate their utility.

2. Absorption by Vapor and by Solution. By standard theory, the transmission coefficient  $T$  of electromagnetic radiation of wavelength  $\lambda = 2\pi c/\omega$  passing through a cell of thickness  $L$  containing a concentration  $x$  of material having a complex refractive index  $\bar{n} = n + ik$  as condensed material, has the following form:

$$T = \exp (-2kx \cdot 2\pi L/\lambda) .$$

Upon taking logarithms and expressing  $\lambda$  in terms of the angular frequency  $2\pi c/\omega$ , we have

$$- \ln T = 2kxL \omega / c = 2xL (\omega_0/c) (\omega/\omega_0) k .$$

To evaluate the adequacy of the theoretical expression for  $k(\omega)$ , we need to calculate  $(\omega/\omega_0)k$  for comparison with  $-\ln T$ . First we calculate  $k$  by eliminating  $n$  between the expressions for  $n^2 - k^2 \equiv A^2$  and  $2nk \equiv B^2$ . The result is

$$k^2 = \frac{1}{2} B^2 / \sqrt{1 + (A^2/B^2)^2} - A^2/B^2 ,$$

a result too complicated to be visualized easily when the full expressions

for  $A^2$  and  $B^2$  as functions of  $\omega$  are inserted. But experiment shows typically that in the neighborhood of the absorption maximum,  $n^2 - k^2 = \epsilon_\infty$  is about 2, where as  $2nk = (\epsilon_0 - \epsilon_\infty)/(\delta/\omega_0)$  is about 100. Hence the term in braces in the expression for  $k^2$  is very nearly equal to unity. In this approximation  $k \cong 1/\sqrt{2} B$ , and

$$\ln\left(\frac{T_\infty}{T}\right) = \sqrt{2} \times L \cdot 2\pi\tilde{\nu}_0 (\tilde{\nu}/\tilde{\nu}_0)^{\frac{1}{2}} \cdot \sqrt{\frac{(\epsilon_0 - \epsilon_\infty)(\delta/\omega_0)}{(\tilde{\nu}_0/\tilde{\nu} - \tilde{\nu}/\tilde{\nu}_0)^2 + (\delta/\omega_0)^2}}$$

Here we have replaced  $T$  by  $T/T_\infty$ , the ratio of the observed transmission at a given  $\tilde{\nu}$  to the transmission far from  $\tilde{\nu}_0$ , since radiation is lost from the beam by effects other than that of the oscillator under study. Inspection of the preceding equation shows that  $\ln (T_\infty/T)$ , which is a measure of the absorption, in the neighborhood of  $\tilde{\nu}_0$  is proportional to the product of a slowly-varying function,  $(\tilde{\nu}/\tilde{\nu}_0)^{\frac{1}{2}}$ , times the rapidly varying function under the radical. The maximum absorption is displaced only slightly from the maximum of the rapidly varying function, which is seen to occur at  $\tilde{\nu} = \tilde{\nu}_0$ . Hence  $\tilde{\nu}_0$  may be obtained by inspection as the abscissa at the minimum of the observed transmission curves.

To reduce some of the experimental scatter, and also to get into position to test the observed curves for adherence to the theoretical formula for  $\epsilon$ , we note that the rapidly varying function is symmetrical in  $\tilde{\nu}/\tilde{\nu}_0$  and its reciprocal. Hence there will be two values of  $\tilde{\nu}$  labeled  $\tilde{\nu}_-$  and  $\tilde{\nu}_+$ , for which  $T/T_\infty$  has the same value. It is easy to show that

$$\tilde{\nu}_- \tilde{\nu}_+ = \tilde{\nu}_0^2$$

according to the theory. Accordingly we plot  $\bar{\nu}_+ \bar{\nu}_-$  against T, expecting to find a horizontal line, or rather a set of points converging to a horizontal line as  $T_{\min}$  is approached. Fig. 33 shows the result of such a procedure. The points converge to a value corresponding to  $\bar{\nu}_0 = 2577 \text{ cm}^{-1}$  which we take as a good estimate of this parameter.

We could now go on to test the form of the equation, by recasting it in the form

$$\left( \frac{\bar{\nu}_+}{\bar{\nu}} - \frac{\bar{\nu}_-}{\bar{\nu}_0} \right)^2 = K \left\{ \frac{\bar{\nu}/\bar{\nu}_0}{[\ln(T/T_\infty)]^2} - \frac{1}{[\ln(T_{\min}/T_\infty)]^2} \right\},$$

where

$$K \equiv 2x^2 L^2 4\pi^2 \bar{\nu}_0^2 (\epsilon_0 - \epsilon_\infty) (\delta/\omega_0).$$

Then a plot of  $(\bar{\nu}_0/\bar{\nu} - \bar{\nu}_-/\bar{\nu}_0)^2$  against  $(\bar{\nu}/\bar{\nu}_0)/[\ln(T/T_\infty)]^2 - 1/[\ln(T_{\min}/T_\infty)]^2$  should give a straight line through the origin with slope K. Such plots have been made but do not agree very well with the straight line predicted. This disagreement may be partially due to the contribution of the rotational motion to the absorption. Further studies must be made, however, before useful information can be gained from the slope of the predicted line.

#### D. Suggestions for Future Studies

The existence of an order-disorder phenomenon in the crystal structure of decaborane suggest that absorption studies be carried out at low temperatures. According to our explanation, the presence of the doublet is based on the environment of the terminal hydrogen

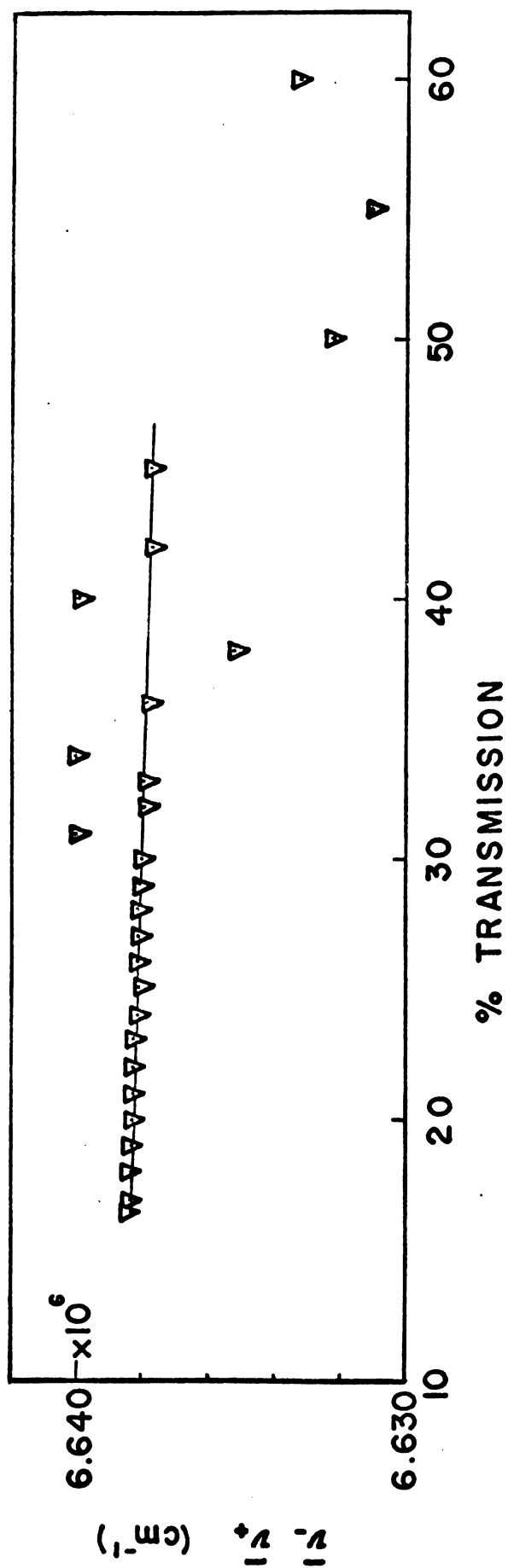


Fig. 33. - Plot of  $\nu_4$  vs transmission T for decaborane vapor.



atoms in the crystal lattice. This environment remains the same when the structure changes from disordered to ordered. Hence the doublet should appear in the spectrum of the solid even at liquid-helium temperature. Our explanation depends primarily on whether the crystal structure is correct in all detail. X-ray determination of a complex structure of poorly-scattering atoms, however, is a formidable problem.

More information concerning environmental effects and the change in absorption accompanying the change in state may be gained by considering the absorption of liquid  $B_{10}H_{14}$ . A suitable liquid sample may be obtained by melting some  $B_{10}H_{14}$  powder between a pair of KBr disks.

A study of the absorption of a thin film of decaborane should be carefully considered beyond  $\lambda = 15\mu$  ( $\tilde{\nu} < 667\text{ cm}^{-1}$ ). Of particular interest is the very-far-infrared region where one may gain information concerning lattice vibrations. In conjunction with the present study, study of the far-infrared region may provide information concerning the interaction of the more or less localized vibrations of the molecules with the vibrations of the lattice. By varying  $B^{10}$  and  $B^{11}$  as well as  $H^1$  and  $H^2$ , isotopic mass may be chosen as the probe for such a study of the lattice vibrations of decaborane.

## BIBLIOGRAPHY

1. M. Born and K. Huang, Dynamical Theory of Crystal Lattices (Oxford at the Clarendon Press, 1954), Chapter 2.
2. W. B. Zimmerman, Ph.D. Thesis, Michigan State University, 1960.
3. W. B. Zimmerman and D. J. Montgomery, Phys. Rev. 120, 405 (1960); Bull. Am. Phys. Soc. 5, 415 (1960).
4. R. H. Misho, Ph.D. Thesis, Michigan State University, 1961.
5. R. H. Misho and D. J. Montgomery, Bull. Am. Phys. Soc. 6, 284, 450 (1961).
6. C. J. Major, Chem. Eng. Progress 54, 49 (1958).
7. Technical Bulletin C-070, Callery Chemical Company.
8. A. Stock, Hydrides of Boron and Silicon (Cornell University Press, 1933), Chapter 10.
9. Technical Bulletin LF-1; Olin-Mathieson Chemical Corporation, March, 1960.
10. J. S. Kasper, C. M. Lucht, and D. Hacker, Acta Cryst. 3, 436 (1950).
11. E. H. Krackow, Toxicity and Health Hazards of Boron Hydrides; Report 113093-U. S. Dept. of Commerce, Office of Technical Services, Washington 25, D. C.
12. H. H. Schrenk, Ind. and Eng. Chem. 49, 87A (1957).
13. W. E. Keller and H. L. Johnston, J. Chem. Phys. 20, 1749 (1952).
14. L. J. Bellamy, Spectrochim. Acta 14, 192 (1954).
15. J. J. Miller and M. F. Hawthorne, J. Amer. Chem. Soc. 81, 4501 (1959).
16. J. C. Beachell, Astin - AD 234979, Progress Report, Jan. 1, 1960, March 31, 1960; Ballistic Research Lab., Army Ordnance Corps, Aberdeen Proving Ground, Maryland.

17. T. A. Kletz and W. C. Price, J. Chem. Soc., 644 (1947).
18. R. P. Bauman, Absorption Spectroscopy (John Wiley & Sons, 1962), Chapter 4.
19. F. A. Miller and C. H. Wilkens, Analytical Chemistry 24, 1255 (1952).
20. A. W. Baker, J. Phys. Chem. 61, 450 (1957).
21. H. J. Hrostowski and G. C. Pimentel, J. Amer. Chem. Soc. 76, 998 (1954).
22. L. J. Bellamy, W. Gerrard, M. F. Lappert, and R. L. Williams, J. Chem. Soc., 2412 (1958).
23. I. Shapiro, C. O. Wilson, and W. J. Lehmann, J. Chem. Phys. 29, 237 (1958).
24. C. Christiansen, Ann. Physik 23, 298 (1884); 24, 439 (1885).
25. R. B. Barnes and L. G. Bonner, Phys. Rev. 49, 732 (1936).
26. C. Kittel, Introduction to Solid State Physics (John Wiley & Sons, Inc., 1961), Chapter 1.
27. F. O. Rice and E. Teller, The Structure of Matter (John Wiley & Sons, Inc., 1949), Chapter 10.
28. M. Born and E. Wolf, Principles of Optics (Pergamon Press, 1959), p. ff.
29. D. J. Montgomery and K. F. Yeung, J. Chem. Phys. 37, 1056 (1962).

MICHIGAN STATE UNIV. LIBRARIES



31293017430160